

Accepted Manuscript

Design, synthesis and biological evaluation of novel 4-aminoquinazolines as dual target inhibitors of EGFR-PI3K α

Huai-Wei Ding, Cheng-Long Deng, Dan-Dan Li, Dan-Dan Liu, Shao-Meng Chai, Wei Wang, Yan Zhang, Kai Chen, Xin Li, Jian Wang, Shao-Jiang Song, Hong-Rui Song



PII: S0223-5234(18)30100-4

DOI: [10.1016/j.ejmech.2018.01.081](https://doi.org/10.1016/j.ejmech.2018.01.081)

Reference: EJMECH 10158

To appear in: *European Journal of Medicinal Chemistry*

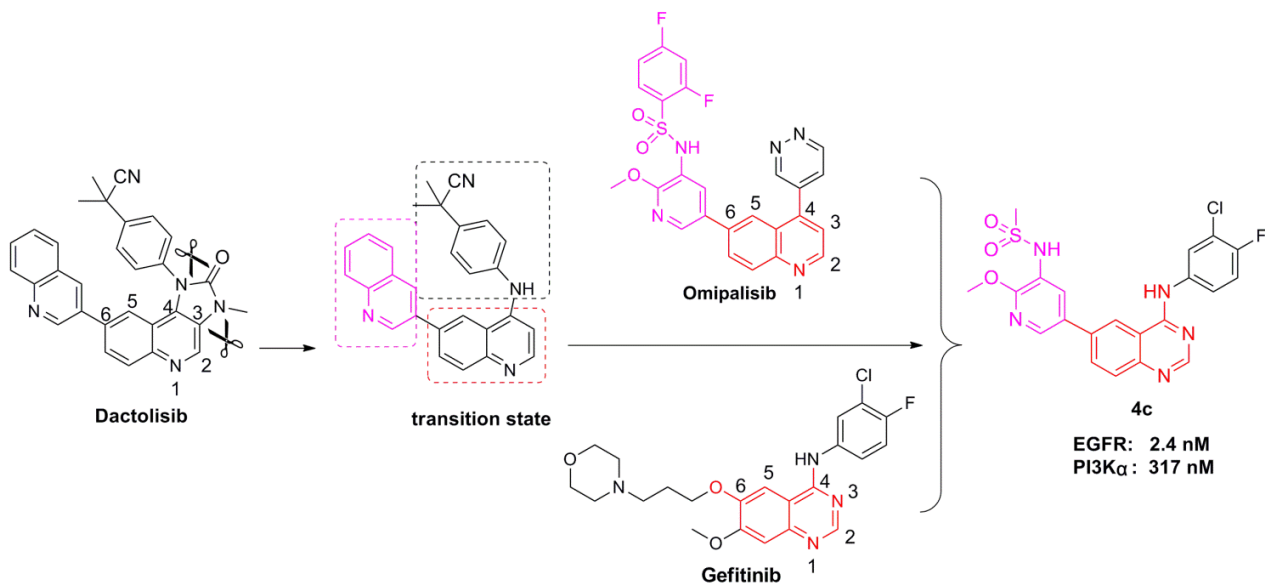
Received Date: 3 August 2017

Revised Date: 22 January 2018

Accepted Date: 24 January 2018

Please cite this article as: H.-W. Ding, C.-L. Deng, D.-D. Li, D.-D. Liu, S.-M. Chai, W. Wang, Y. Zhang, K. Chen, X. Li, J. Wang, S.-J. Song, H.-R. Song, Design, synthesis and biological evaluation of novel 4-aminoquinazolines as dual target inhibitors of EGFR-PI3K α , *European Journal of Medicinal Chemistry* (2018), doi: 10.1016/j.ejmech.2018.01.081.

This is a PDF file of an unedited manuscript that has been accepted for publication. As a service to our customers we are providing this early version of the manuscript. The manuscript will undergo copyediting, typesetting, and review of the resulting proof before it is published in its final form. Please note that during the production process errors may be discovered which could affect the content, and all legal disclaimers that apply to the journal pertain.



Design, synthesis and biological evaluation of novel 4-aminoquinazolines as dual target

inhibitors of EGFR-PI3K α

Huai-Wei Ding^a, Cheng-Long Deng^a, Dan-Dan Li^b, Dan-Dan Liu^a, Shao-Meng Chai^c, Wei Wang^b, Yan Zhang^b, Kai Chen^a, Xin Li^b, Jian Wang^a, Shao-Jiang Song^b, Hong-Rui Song^{a,*}

^a Key Laboratory of Structure-Based Drug Design and Discovery, Ministry of Education, Shenyang Pharmaceutical University, Shenyang 110016, China

^b School of Traditional Chinese Materia Medica, Shenyang Pharmaceutical University, Shenyang 110016, China

^c Key Laboratory for Molecular Enzymology & Engineering, Jilin University, China

* Corresponding authors.

Email address: hongruisong@163.com.

Abstract: The overexpression of EGFR correlates with rapidly progressive disease, resistance to chemotherapy and poor prognosis. In certain human cancers, PI3K works synergistically with EGFR to promote proliferation, survival, invasion and metastasis. Development of dual-target drugs against EGFR and PI3K has therapeutic advantage and was an attractive approach against tumors. In this work, based on the molecular docking and previous studies, a series of 4-aminoquinazolines derivatives containing 6-sulfonamide substituted pyridyl group were rationally designed and identified as potent EGFR and PI3K dual inhibitors. The cytotoxicity experiment results showed that this series of compounds could effectively inhibit cell growth. The kinase assay demonstrated that **6c** and **6i** had high inhibition for EGFR and selectivity for PI3K α distinguished from other isoforms. Further experiments showed that **6c** could induce cell cycle arrest in G1 phase and apoptosis in BT549 cells. The western blot assay indicated that **6c** inhibited the proliferation of BT549 cell through EGFR and PI3K α /Akt signaling pathway. Our study suggested that compound **6c** was a potential dual inhibitors of EGFR and PI3K α .

Keywords: EGFR, PI3K, dual target, 4-aminoquinazolines, antiproliferative effects, anticancer agents

The epidermal growth factor receptor (EGFR) belongs to the ErbB family of receptor tyrosine kinase, which includes four members: ErbB-1/EGFR, ErbB-2/HER-2/neu, ErbB-3/HER-3, and ErbB-4/HER-4 [1-2]. The overexpression of EGFR activates a series of downstream signals via several pathways and leads to tumor growth and progression, including proliferation, differentiation, angiogenesis, inhibition of apoptosis and invasiveness. The major pathways implicated in EGFR signaling include RAS/MAPK, PI3K/Akt, and JAK/STAT [3-5]. A lot of inhibitors targeting EGFR have been successfully developed and contain six launched drugs, Gefitinib [6], Lapatinib [7], Erlotinib [8], Vandetanib [9], Afatinib [10] and Icotinib [11] (Fig.1).

The phosphatidylinositol 3-kinases (PI3Ks) are members of a unique group of intracellular lipid kinases [12]. The PI3K family is divided into four different classes: Class I, Class II, Class III and Class IV. The classifications are based on the primary structure, regulation, and *in vitro* lipid substrate specificity. Of these, the most commonly studied are the class I enzymes that are activated directly by cell surface receptors. Class I PI3Ks are further divided into PI3K α , PI3K β , PI3K δ and PI3K γ [13-14]. The abnormal activation of PI3K signaling pathway leads to the occurrence of various cancers [15], suggesting that targeting inhibition of PI3K may be a potential strategy against cancer. Several inhibitors targeting PI3K have been developed and are being evaluated in preclinical studies and early clinical trials [16-17]. Among them, Omipalisib (GSK2126458) and Dactolisib (NVP-BEZ235) has been identified as highly potent inhibitors of PI3K and are currently under evaluation in clinical trials for oncology applications [18-19] (Fig.2).

Quinazoline derivatives, especially 4-anilinoquinazolines, have attracted interests over the years for their multiple biological activities, notably as EGFR inhibitors [20]. In recent years, 4-aminoquinazoline derivatives also have been reported as PI3K inhibitors [21-23]. We had a good understanding of the binding mode of Gefitinib and Omipalisib based on the reported corresponding X-ray structure of kinase domain [18, 24]. Gefitinib and Omipalisib all using the position-1 nitrogen as a hinge binder and all having an aryl group at the position-4, we hypothesized that we would gain dual target compounds by adjusting the substituent groups of molecules. Coincidentally, we found that Dactolisib could be cut off the N-methyl formamide group to obtain a "transition state" (Fig.2), which had structural similarity to Gefitinib and Omipalisib. This discovery further encourages the development of our work to design dual inhibitors. In this paper, as an attempt to pursue new antitumor agents potently inhibiting both EGFR and PI3K α , we rationally designed and synthesized a new series of 4-aminoquinazolines derivatives from Gefitinib, Omipalisib and Dactolisib (Fig.2). The biological activities evaluation suggest that compound **6c** and **6i** could be as dual inhibitors of EGFR and PI3K α .

(Fig. 1. is here)

2. Results and discussion

2.1. Chemistry

The synthetic routes for the target compounds are outlined in Schemes 1. Sulfonylation of **1** with three benzenesulfonyl chlorides to yield **2a-c**, which were then subjected to Suzuki coupling with bis(pinacolato)diborane to afford arylboronic ester **3a-c**. Intermediate **4** reacted with different substituted anilines to obtain **5a-p**, which were coupled with **3a-c** via Suzuki reaction to afford the target compounds **6a-r**.

(Scheme 1. is here)

2.2. Antiproliferative assays *in vitro*

All synthesized compounds were evaluated for their cytotoxicities *in vitro* against six human cancer cell lines including A549, BT549, HCT-116, MCF-7, SK-HEP-1 and SNU638 cells. The antiproliferative results of all the compounds were summarized in Table 1. As shown in Table 1, the results showed that most of the derivatives exhibited potent antiproliferative effects. The structure-activity relationships (SARs) suggested that all of compounds with methyl substituent on R₂ position displayed better antiproliferative activities than those substituted by N-butyl or phenyl group on the same position, including **6a-m** vs. **6n-p**. Especially from representative compounds **6i**, **6o** and **6p**, gave the hints that the larger the volume of sulfonamide, the worse the activity. Compounds **6b-d** and **6f-l** mainly showed better activities against six cell lines than Gefitinib, but weaker than Dactolisib. In order to let target compounds closer to GSK2126458, nitrogen atoms were introduced in the position-3' of the 4-anilinoquinazolines to get the compound **6q** and **6r**. Interestingly, the activity was not increased but decreased, including **6b** vs. **6q** and **6f** vs. **6r**.

(Table 1 is here)

2.3. EGFR and PI3K enzymatic activity assays

To elucidate the mechanism of antiproliferative activities of these active compounds, we selected the most potent compounds **6c** and **6i** for the further EGFR and PI3K enzymatic activity assays. Gefitinib and Dactolisib were selected as the positive drugs. As shown in Table 2, kinase inhibition activity assay indicated that the activity of **6c** and **6i** has reached the nanomolar level. Two compounds above showed a higher inhibitory activity against PI3K α when compared to that of other class I PI3Ks (PI3K β , PI3K γ and PI3K δ). Coincidentally, the EGFR inhibitory activity of **6c** was basically equal to Gefitinib.

(Table 2 is here)

Considering to the structure similarity to Gefitinib, the antiproliferative results and the BT549 cells presenting more sensitive to this series of compounds, we selected compound **6c** and BT549 cells for further studies.

2.4. Effect of **6c** on the growth of BT549 cells

ACCEPTED MANUSCRIPT

In order to further investigate the antiproliferation of **6c** on BT549 cells, the colony formation assay was used to measure the cell viability. As shown in Fig.3, the cell proliferation was inhibited by **6c** in a dose-dependent manner. Analyzing of the clonogenicity viability, the colony formation rate of 2.5 μM was 55.6% more than 25.7% of 5.0 μM . Compared with control group, **6c** almost completely inhibited colony formation at a concentration of 5.0 μM . The results of antiproliferative assay and colony formation assay suggested that **6c** can inhibit the proliferation of BT549 cells prominently.

(Fig. 3. is here)

2.5. Apoptosis induced by compound **6c**

Though **6c** was proved antitumor effects, the mechanism was not clear. Annexin V-PI double staining assay was used to examine the effect of **6c** on cells apoptosis. As shown in Fig.4 (A and B), **6c** can induce apoptosis compared with control. The percentage of late apoptotic at 5.0 μM was more than at 1.0 μM , it is indicated that **6c** induced the early apoptotic transform to late apoptotic following with the alternative concentration.

In order to further evaluate **6c**-induced apoptosis in BT549 cells, cells were staining with DAPI and analyzing by fluorescence microscope. As shown in Fig.4 (C), treated with different concentrations of **6c**, the brighter fluorescence was seen. Compared with control which had normal nuclear morphology after DAPI staining, **6c** treatment group marked with nuclear fragmentation and condensation of chromatin. Moreover, this situation was more obvious with the increased concentration. These results indicated that **6c** was capable of inducing apoptosis in BT549 cells.

(Fig. 4. is here)

2.6. Effect of compound **6c** on cell cycle

To determine whether inhibitory effect of **6c** on the cell survival was related to the cell cycle, propidium iodide(PI) staining assay was used. After treatment with **6c** for 24 h, as shown in Fig.4 (D and E), the percentage of G1 phase was increased obviously and had a dose-dependent manner. The arrested G1 phase ratio increased from 55.9% to 80.7% with increasing **6c** concentration from 0 μM to 5.0 μM . This result showed that **6c** induce cell cycle arrest in G1 phase.

2.7. Western blot assay

To further determine whether the EGFR and PI3K signaling were affected by compound **6c**, Western blot assay was used to evaluate the effects of **6c** on EGFR and phospho-EGFR and the PI3K related protein levels including Akt and phospho-Akt (p-Akt, S473) in BT549 cells. As shown in Fig.5 (A and B), compound **6c** decreased the phosphorylation levels of EGFR and Akt in a dose-dependent manner. The rate of p-EGFR/EGFR and p-Akt/Akt was down-regulated by **6c**. Therefore, the data suggested that **6c** might

inhibit the proliferation of BT549 cell through EGFR and Akt signaling pathway.

(Fig. 5. is here)

2.8. Molecular docking

Molecular docking study was performed to elucidate the binding model of **6c** in the binding site of EGFR and PI3K. As showed in Fig.6 (A), the nitrogen of quinazolyl group formed a hydrogen bond with the side chain of Met793 in the hinge binder region of EGFR. Besides, the amidogen of sulfonamide group forms extra two hydrogen bond interaction with Arg841 and Leu799 compare to Gefitinib. By Fig.6 (B), we know that the folded form of compound **6c** in the protein pocket was very similar to that of Gefitinib. Compound **6c** was also docked onto the PI3K-binding domain. The structure of PI3K kinase was obtained from protein data bank (PDB entry 3L08). The Fig.6 (C) showed that the ligand **6c** formed three strong hydrogen bonds. The nitrogen of quinazolyl group formed a hydrogen bond with the side chain of Val882 in the hinge binder region of PI3K. Another two hydrogen bonds were the oxygen of sulfonamide group interaction with Lys833 and nitrogen of pyridyl group formed a hydrogen bond with the conserved water molecule. As showed in Fig.6 (D), the folded form of compound **6c** in the protein pocket was very similar to that of Omipalisib.

The docking analysis indicated that compound **6c** could fit into the binding site of EGFR and PI3K kinases, which also indicated that this compound may be a potent EGFR and PI3K inhibitor.

(Fig. 6. is here)

3. Conclusion

In summary, a series of compounds containing 4-aminoquinazolines were designed and synthesized. Their antiproliferative activities against six cancer cell lines showed that the BT549 cells presented more sensitive to these compounds. Eventually, compound **6c** and BT549 cells were selected for further research. Thereafter, in order to identify the antiproliferation of **6c** on BT549 cells, the colony formation assay and apoptosis were evaluated *in vitro*. The results suggested that **6c** could inhibit the proliferation of BT549 cells prominently and induce the early apoptotic transform to late apoptotic following with the alterative concentration. In order to verify the further mechanisms of **6c**, the propidium iodide (PI) staining assay was developed and the results showed that **6c** arrested G1 phase of cell cycle. we also conducted Western-blot experiment and the results showed that **6c** inhibited the proliferation of BT549 cell through EGFR and PI3K α /Akt signaling pathway. According to these results, compound **6c** could be as a potential EGFR/PI3K α dual target inhibitor and could be considered as a potential candidate for anticancer drug development.

4. Experimental section

4.1. Chemistry and chemical methods

ACCEPTED MANUSCRIPT

All reagents and solvents were commercially available without further purification. ^1H NMR spectra and ^{13}C NMR spectra were recorded on 400 and 600 Bruker NMR spectrometer with tetramethylsilane (TMS) as an internal standard. All chemical shifts are reported in ppm (δ) and coupling constants (J) are in hertz (Hz). All the melting points were determined on a Beijing micromelting-point apparatus and thermometer was uncorrected. High-resolution exact mass measurements were performed using electrospray ionization (positive mode) on a quadrupole time-of-flight (QTOF) mass spectrometer (microTOF-Q, Bruker Inc.).

4.1.1. *N*-(5-bromo-2-methoxy-pyridin-3-yl)butane-1-sulfonamide (**2a**)

To a solution of 5-bromo-2-methoxy-pyridin-3-amine (2.01 g, 10 mmol) in pyridine (50 ml) at 0 °C was added methanesulfonyl chloride (1.72 g, 11 mmol). Then the mixture was stirred at room temperature 24 h. Pyridine was removed at reduced pressure and add water (100 ml), extracted with ethyl acetate (3 \times 100 ml), the organic layer was washed with water (50 ml), dried with Na_2SO_4 and evaporated to give compound **2a** as a white solid. Yield 83.6%, mp 150-151 °C. ^1H NMR (400 DMSO- d_6) δ 9.49 (s, 1H, NH), 8.09 (d, J = 2.4 Hz, 1H, Ar-H), 7.79 (d, J = 2.0 Hz, 1H, Ar-H), 3.91 (s, 3H, OCH_3), 3.11 (s, 3H, CH_3). ESI-MS: m/z 281.1 $[\text{M}+\text{H}]^+$.

Compounds **2b-c** was synthesized according to the procedure described in **2a**.

4.1.2. *N*-(5-bromo-2-methoxy-pyridin-3-yl)butane-1-sulfonamide (**2b**)

78.4% yield. mp 150-151 °C. ^1H NMR (400 MHz, DMSO- d_6) δ 9.51 (s, 1H, NH), 8.09 (d, J = 2.4 Hz, 1H, Ar-H), 7.77 (d, J = 2.4 Hz, 1H, Ar-H), 3.91 (s, 3H, OCH_3), 3.16 (t, J = 7.6 Hz, 2H, CH_2), 1.73 - 1.65 (m, 2H, CH_2), 1.42 - 1.33 (m, 2H, CH_2), 0.87 (t, J = 7.2 Hz, 3H, CH_3). ESI-MS: m/z 323.1 $[\text{M}+\text{H}]^+$.

4.1.3. *N*-(5-bromo-2-methoxy-pyridin-3-yl)-2,4-difluorobenzenesulfonamide (**2c**)

85.6% yield. mp 163-165 °C. ^1H NMR (400 MHz, DMSO) δ 10.46 (s, 1H, NH), 8.13 (d, J = 2.2 Hz, 1H, Ar-H), 7.83-7.74 (m, 2H, Ar-H), 7.62-7.52 (m, 1H, Ar-H), 7.24 (td, J = 2.0, 8.5 Hz, 1H, Ar-H), 3.62 (s, 3H, OCH_3). ESI-MS: m/z 376.9 $[\text{M}+\text{H}]^+$.

4.1.4. *N*-(2-methoxy-5-(4,4,5,5-tetramethyl-1,3,2-dioxaborolan-2-yl)pyridin-3-yl)methanesulfonamide (**3a**)

A solution of the **2a** (2.80 g, 10 mmol), bis(pinacolato)diborane (1.27 g, 5 mmol), $\text{Pd}(\text{dppf})_2\text{Cl}_2$ (0.18 g, 0.25 mmol) and KOAc (1.47 g, 15 mmol) in anhydrous DMF (30 ml) under N_2 was stirred at 100 °C for 8 h. DMF was removed under reduced pressure and add water (100 ml), extracted with ethyl acetate (3 \times 100 ml), the organic layer was washed with water (20 ml), dried with Na_2SO_4 and evaporated to give compound **3a** as a white solid (1.98 g, 60.4% yield). mp 90-92 °C. ^1H NMR (400 MHz, DMSO) δ 9.25 (s, 1H, NH), 8.21 (d, J = 1.6 Hz, 1H, Ar-H), 7.78 (d, J = 1.6 Hz, 1H, Ar-H), 3.94 (s, 3H, OCH_3), 3.01 (s, 3H, CH_3), 1.30 (s, 12H, CH_3). ESI-MS: m/z 329.1 $[\text{M}+\text{H}]^+$.

Compounds **3b-c** were synthesized according to the procedure described in **3a**.

4.1.5. *N*-(2-methoxy-5-(4,4,5,5-tetramethyl-1,3,2-dioxaborolan-2-yl)pyridin-3-yl)butane-1-sulfonamide (**3b**)

64.3% yield. mp 91-93 °C. ¹H NMR (400 MHz, DMSO) δ 9.26 (s, 1H, NH), 8.21 (d, *J* = 1.4 Hz, 1H, Ar-H), 7.79 (d, *J* = 1.3 Hz, 1H, Ar-H), 3.94 (s, 3H, OCH₃), 3.10 - 3.01 (m, 2H, CH₂), 1.76 - 1.63 (m, 2H, CH₂), 1.38 (dt, *J* = 7.4, 14.8 Hz, 2H, CH₂), 1.30 (s, 12H, CH₃), 0.86 (t, *J* = 7.3 Hz, 3H, CH₃). ESI-MS: *m/z* 371.2 [M+H]⁺.

4.1.6.

2,4-difluoro-*N*-(2-methoxy-5-(4,4,5,5-tetramethyl-1,3,2-dioxaborolan-2-yl)pyridin-3-yl)benzenesulfonamide (**3c**)

78.8% yield. mp 171-173 °C. ¹H NMR (400 MHz, DMSO) δ 10.19 (s, 1H, NH), 8.21 (d, *J* = 1.5 Hz, 1H, Ar-H), 7.72 (d, *J* = 1.5 Hz, 1H, Ar-H), 7.71-7.67 (m, 1H, Ar-H), 7.59-7.54 (m, 1H, Ar-H), 7.20 (td, *J* = 2.0, 8.6 Hz, 1H, Ar-H), 3.62 (s, 3H, OCH₃), 1.30 (s, 12H, CH₃). ESI-MS: *m/z* 427.3 [M+H]⁺

4.1.7. 6-bromo-*N*-(3-fluorophenyl)quinazolin-4-amine (**5a**)

A solution of the **4** (0.48 g, 2 mmol), 3-fluoroaniline (0.24g, 2.2 mmol) in isopropanol (30 ml) were stirred at 90 °C for 4 h. Isopropanol was removed under reduced pressure and the residue was purified through a column chromatography on silica with chloroform/methanol (V:V 50:1) as a white solid (0.58 g, 91.8% yield). mp 167-169 °C. ¹H NMR (400 MHz, DMSO) δ 12.05 (s, 1H, NH), 9.45 (s, 1H, Ar-H), 9.03 (s, 1H, Ar-H), 8.26 (d, *J* = 8.9 Hz, 1H, Ar-H), 8.02 (d, *J* = 8.9 Hz, 1H, Ar-H), 7.78 (d, *J* = 10.9 Hz, 1H, Ar-H), 7.67 (d, *J* = 8.1 Hz, 1H, Ar-H), 7.53 (dd, *J* = 15.1, 8.0 Hz, 1H, Ar-H), 7.18 (td, *J* = 8.4, 1.8 Hz, 1H, Ar-H). ESI-MS: *m/z* 315.9 [M-H]⁺.

Compounds **5b-p** were synthesized according to the procedure described in **5a**.

4.1.8. 6-bromo-*N*-(4-fluorophenyl)quinazolin-4-amine (**5b**)

90.6% yield. mp 228-230 °C. ¹H NMR (400 MHz, DMSO) δ 11.01 (s, 1H, NH), 9.15 (d, *J* = 1.5 Hz, 1H, Ar-H), 8.77 (s, 1H, Ar-H), 8.10 (dd, *J* = 8.9, 1.7 Hz, 1H, Ar-H), 7.84 (dd, *J* = 8.7, 6.1 Hz, 3H, Ar-H), 7.29 (t, *J* = 8.8 Hz, 2H, Ar-H). ESI-MS: *m/z* 315.9 [M-H]⁺.

4.1.9. 6-bromo-*N*-(2,4-difluorophenyl)quinazolin-4-amine (**5c**)

88.9% yield. mp 197-199 °C. ¹H NMR (400 MHz, DMSO) δ 10.55 (s, 1H, NH), 8.89 (d, *J* = 1.8 Hz, 1H, Ar-H), 8.64 (s, 1H, Ar-H), 8.09 (dd, *J* = 8.9, 2.0 Hz, 1H, Ar-H), 7.80 (d, *J* = 8.9 Hz, 1H, Ar-H), 7.58 (td, *J* = 8.8, 6.3 Hz, 1H, Ar-H), 7.46 - 7.41 (m, 1H, Ar-H), 7.25 - 7.15 (m, 1H, Ar-H). ESI-MS: *m/z* 333.9 [M+H]⁺.

4.1.10. 6-bromo-*N*-(3-chloro-4-fluorophenyl)quinazolin-4-amine (**5d**)

94.4% yield. mp 229-231 °C. ¹H NMR (400 MHz, DMSO) δ 11.92 (s, 1H, NH), 9.34 (d, *J* = 1.1 Hz, 1H, Ar-H), 9.34 (d, *J* = 1.1 Hz, 1H, Ar-H), 9.00 (s, 1H, Ar-H), 8.25 (dd, *J* = 8.8, 1.4 Hz, 1H, Ar-H), 8.09 (dd, *J* = 6.7, 2.3 Hz, 1H, Ar-H), 7.97 (d, *J* = 8.9 Hz, 1H, Ar-H), 7.80 (ddd, *J* = 8.6, 4.0, 2.7 Hz, 1H, Ar-H), 7.56 (t, *J* = 9.0 Hz, 1H, Ar-H). ESI-MS: *m/z* 351.9 [M+H]⁺.

4.1.11. 6-bromo-N-(4-(trifluoromethoxy)phenyl)quinazolin-4-amine (**5e**)

96.1% yield. mp 178-180 °C. ¹H NMR (400 MHz, DMSO) δ 11.90 (s, 1H, NH), 9.34 (d, *J* = 1.7 Hz, 1H, Ar-H), 8.97 (s, 1H, Ar-H), 8.26 (dd, *J* = 8.9, 1.8 Hz, 1H, Ar-H), 7.97 (d, *J* = 8.9 Hz, 1H, Ar-H), 7.90 (d, *J* = 9.0 Hz, 2H, Ar-H), 7.51 (d, *J* = 8.5 Hz, 2H, Ar-H). ESI-MS: *m/z* 381.8 [M-H]⁺.

4.1.12. 6-bromo-N-(4-methoxyphenyl)quinazolin-4-amine (**5f**)

86.2% yield. mp 195-197 °C. ¹H NMR (400 MHz, DMSO) δ 11.72 (s, 1H, NH), 9.27 (s, 1H, Ar-H), 8.89 (s, 1H, Ar-H), 8.22 (d, *J* = 8.8 Hz, 1H, Ar-H), 7.95 (d, *J* = 8.9 Hz, 1H, Ar-H), 7.65 (d, *J* = 8.8 Hz, 2H, Ar-H), 7.05 (d, *J* = 8.9 Hz, 2H, Ar-H), 3.81 (s, 3H, OCH₃). ESI-MS: *m/z* 330.1 [M+H]⁺.

4.1.13. 6-bromo-N-(3,4-dimethoxyphenyl)quinazolin-4-amine (**5g**)

87.5% yield. mp 183-185 °C. ¹H NMR (400 MHz, DMSO) δ 11.67 (s, 1H, NH), 9.26 (d, *J* = 1.3 Hz, 1H, Ar-H), 8.92 (s, 1H, Ar-H), 8.23 (dd, *J* = 8.8, 1.7 Hz, 1H, Ar-H), 7.94 (d, *J* = 8.9 Hz, 1H, Ar-H), 7.40 (d, *J* = 2.2 Hz, 1H, Ar-H), 7.33 (dd, *J* = 8.6, 2.2 Hz, 1H, Ar-H), 7.06 (d, *J* = 8.7 Hz, 1H, Ar-H), 3.81 (s, 3H, OCH₃), 3.78 (s, 3H, OCH₃). ESI-MS: *m/z* 360.1 [M+H]⁺.

4.1.14. 6-bromo-N-(3-chloro-4-methoxyphenyl)quinazolin-4-amine (**5h**)

91.4% yield. mp 260-262 °C. ¹H NMR (400 MHz, DMSO) δ 10.13 (s, 1H, NH), 8.91 (d, *J* = 1.7 Hz, 1H, Ar-H), 8.66 (s, 1H, Ar-H), 8.00 (dd, *J* = 5.7, 2.2 Hz, 2H, Ar-H), 7.77 - 7.73 (m, 2H, Ar-H), 7.21 (d, *J* = 9.0 Hz, 1H, Ar-H), 3.88 (s, 3H, OCH₃). ESI-MS: *m/z* 361.8 [M+H]⁺.

4.1.15. 6-bromo-N-(6-fluoropyridin-3-yl)quinazolin-4-amine (**5i**)

85.2% yield. mp 197-199 °C. ¹H NMR (400 MHz, DMSO) δ 10.65 (s, 1H, NH), 9.07 (dd, *J* = 7.8, 1.9 Hz, 1H, Ar-H), 8.69 (s, 2H, Ar-H), 8.48 - 8.44 (m, 1H, Ar-H), 8.05 (dd, *J* = 8.8, 1.8 Hz, 1H, Ar-H), 7.79 (d, *J* = 8.9 Hz, 1H, Ar-H), 7.27 (dd, *J* = 8.7, 3.1 Hz, 1H, Ar-H). ESI-MS: *m/z* 316.8 [M-H]⁺.

4.1.16. 6-bromo-N-(6-methoxypyridin-3-yl)quinazolin-4-amine (**5j**)

87.3% yield. mp 180-182 °C. ¹H NMR (400 MHz, DMSO) δ 11.61 (s, 1H, NH), 9.19 (s, 1H, Ar-H), 8.89 (s, 1H, Ar-H), 8.50 (d, *J* = 2.5 Hz, 1H, Ar-H), 8.22 (dd, *J* = 8.9, 1.7 Hz, 1H, Ar-H), 8.05 (dd, *J* = 8.8, 2.6 Hz, 1H, Ar-H), 7.91 (d, *J* = 8.9 Hz, 1H, Ar-H), 6.96 (d, *J* = 8.9 Hz, 1H, Ar-H), 3.90 (s, 3H, OCH₃). ESI-MS: *m/z* 331.1 [M+H]⁺.

4.1.17. methyl 3-((6-bromoquinazolin-4-yl)amino)benzoate (**5k**)

95.6% yield. mp 218-220 °C. ¹H NMR (400 MHz, DMSO) δ 11.40 (s, 1H, NH), 9.19 (s, 1H, Ar-H), 8.93 (s, 1H, Ar-H), 8.39 (s, 1H, Ar-H), 8.21 (dd, *J* = 8.9, 1.7 Hz, 1H, Ar-H), 8.15 (dd, *J* = 8.0, 0.9 Hz, 1H, Ar-H), 7.91 (d, *J* = 8.9 Hz, 1H, Ar-H), 7.87 (d, *J* = 7.8 Hz, 1H, Ar-H), 7.64 (t, *J* = 7.9 Hz, 1H, Ar-H), 3.90 (s, 3H, OCH₃). ESI-MS: *m/z* 358.1 [M+H]⁺.

4.1.18. ethyl 3-((6-bromoquinazolin-4-yl)amino)benzoate (**5l**)

94.7% yield. mp 196-198 °C. ¹H NMR (400 MHz, DMSO) δ 12.04 (s, 1H, NH), 9.39 (d, *J* = 1.8 Hz, 1H, Ar-H), 9.01 (s, 1H, Ar-H), 8.34 (s, 1H, Ar-H), 8.26 (dd, *J* = 8.9, 1.9 Hz, 1H, Ar-H), 8.10 (dd, *J* = 8.1, 0.9 Hz, 1H, Ar-H), 8.02 (d, *J* = 8.9 Hz, 1H, Ar-H), 7.89 (d, *J* = 7.9 Hz, 1H, Ar-H), 7.64 (t, *J* = 7.9 Hz, 1H, Ar-H), 4.36 (q, *J* = 7.1 Hz, 2H, CH₂), 1.35 (t, *J* = 7.1 Hz, 3H, CH₃). ESI-MS: *m/z* 372.1 [M+H]⁺.

4.1.19. methyl 5-((6-bromoquinazolin-4-yl)amino)-2-fluorobenzoate (**5m**)

81.6% yield. mp 178-180 °C. ¹H NMR (400 MHz, DMSO) δ 11.23 (s, 1H, NH), 9.11 (d, *J* = 1.6 Hz, 1H, Ar-H), 8.89 (s, 1H, Ar-H), 8.30 (dd, *J* = 6.5, 2.7 Hz, 1H, Ar-H), 8.17 (ddd, *J* = 8.8, 7.9, 2.8 Hz, 2H, Ar-H), 7.87 (d, *J* = 8.9 Hz, 1H, Ar-H), 7.54 - 7.44 (m, 1H, Ar-H), 3.91 (d, *J* = 8.0 Hz, 3H, OCH₃). ESI-MS: *m/z* 376.1 [M+H]⁺.

4.1.20. methyl 5-((6-bromoquinazolin-4-yl)amino)-2-chlorobenzoate (**5n**)

84.3% yield. mp 185-187 °C. ¹H NMR (400 MHz, DMSO) δ 11.70 (s, 1H, NH), 9.25 (s, 1H, Ar-H), 9.00 (s, 1H, Ar-H), 8.32-8.24 (m, 2H, Ar-H), 8.08 (d, *J* = 8.8 Hz, 1H, Ar-H), 7.95 (d, *J* = 7.8 Hz, 1H, Ar-H), 7.72 (d, *J* = 8.3 Hz, 1H, Ar-H), 3.91 (s, 3H, OCH₃). ESI-MS: *m/z* 392.1 [M+H]⁺.

4.1.21. methyl 4-((6-bromoquinazolin-4-yl)amino)-2-methoxybenzoate (**5o**)

93.5% yield. mp 165-167 °C. ¹H NMR (400 MHz, DMSO) δ 11.63 (s, 1H, NH), 9.31 (s, 1H, Ar-H), 9.03 (s, 1H, Ar-H), 8.25 (dd, *J* = 8.9, 1.9 Hz, 1H, Ar-H), 7.97 (d, *J* = 8.9 Hz, 1H, Ar-H), 7.79 (d, *J* = 8.5 Hz, 1H, Ar-H), 7.73 (d, *J* = 1.6 Hz, 1H, Ar-H), 7.61 (dd, *J* = 8.5, 1.8 Hz, 1H, Ar-H), 3.87 (s, 3H, OCH₃), 3.81 (s, 3H, OCH₃). ESI-MS: *m/z* 388.1 [M+H]⁺.

4.1.22. 6-bromo-*N*-(3-chloro-4-((4-fluorobenzyl)oxy)phenyl)quinazolin-4-amine (**5p**)

90.7% yield. mp 224-226 °C. ¹H NMR (400 MHz, DMSO) δ 11.53 (s, 1H, NH), 9.23 (s, 1H, Ar-H), 8.91 (s, 1H, Ar-H), 8.20 (dd, *J* = 8.9, 1.7 Hz, 1H, Ar-H), 7.95 (d, *J* = 2.4 Hz, 1H, Ar-H), 7.91 (d, *J* = 8.9 Hz, 1H, Ar-H), 7.70 (dd, *J* = 8.9, 2.4 Hz, 1H, Ar-H), 7.55 (dd, *J* = 8.3, 5.7 Hz, 2H, Ar-H), 7.35 (d, *J* = 9.0 Hz, 1H, Ar-H), 7.26 (t, *J* = 8.8 Hz, 2H, Ar-H), 5.25 (s, 2H, CH₂). ESI-MS: *m/z* 458.0 [M+H]⁺.

4.1.23. *N*-(5-(4-((6-fluoropyridin-3-yl)amino)quinazolin-6-yl)-2-methoxypyridin-3-yl)methanesulfonamide (**6a**)

A solution of the **3a** (0.164 g, 0.5 mmol), **5a** (0.158 g, 0.5 mmol), Pd(dppf)₂Cl₂ (0.018 g, 0.025 mmol) and Cs₂CO₃ (0.33 g, 0.56 mmol) in DMF (10 ml) under an atmosphere of N₂ was stirred at 90 °C for 4 h. DMF was removed under reduced pressure and the residue was purified through a column chromatography on silica with chloroform/methanol (V:V 50:1) as a white solid (0.12 g, 68.2% yield). mp 152-154 °C. ¹H NMR (400 MHz, DMSO) δ 10.02 (s, 1H, NH), 9.53 (s, 1H, NH), 8.83 (s, 1H, Ar-H), 8.68 (s, 1H, Ar-H), 8.53 (s, 1H, Ar-H), 8.18 (d, *J* = 8.4 Hz, 1H, Ar-H), 8.09 (s, 1H, Ar-H), 7.95 (d, *J* = 11.9 Hz, 1H, Ar-H), 7.90 (d, *J* = 8.6 Hz, 1H, Ar-H), 7.69 (d, *J* = 7.8 Hz, 1H, Ar-H), 7.52 - 7.36 (m, 1H, Ar-H), 6.98 (t, *J* = 7.2 Hz, 1H, Ar-H), 4.01 (s, 3H, OCH₃), 3.11 (s, 3H, CH₃). ¹³C NMR (100 MHz, DMSO) δ 162.5 (d, *J* = 239.4 Hz), 158.0,

157.3, 154.8, 149.6, 141.6, 141.4 (d, $J = 5.6$ Hz), 135.3, 132.2, 132.0, 130.5 (d, $J = 9.1$ Hz), 129.4, 129.2, 122.3, 120.7, 118.3 (d, $J = 2.3$ Hz), 115.9, 110.5 (d, $J = 20.6$ Hz), 109.4 (d, $J = 25.8$ Hz), 54.3, 41.3. HRMS (ESI₊) m/z calcd for C₂₁H₁₉FN₅O₃S [M+H]⁺, 440.1187; found, 440.1191.

Compounds **6b-r** was synthesized according to the procedure described in **6a**.

4.1.24. *N*-(5-(4-((4-fluorophenyl)amino)quinazolin-6-yl)-2-methoxy-pyridin-3-yl)methanesulfonamide (**6b**)

64.3% yield, mp 157-159 °C. ¹H NMR (400 MHz, DMSO) δ 9.98 (s, 1H, NH), 9.46 (s, 1H, NH), 8.81 (s, 1H, Ar-H), 8.59 (s, 1H, Ar-H), 8.55 (d, $J = 2.1$ Hz, 1H, Ar-H), 8.17 (d, $J = 8.7$ Hz, 1H, Ar-H), 8.11 (d, $J = 2.1$ Hz, 1H, Ar-H), 7.95 - 7.80 (m, 3H, Ar-H), 7.27 (t, $J = 8.7$ Hz, 2H, Ar-H), 4.02 (s, 3H, OCH₃), 3.13 (s, 3H, CH₃). ¹³C NMR (100 MHz, DMSO) δ 159.1 (d, $J = 238.8$ Hz), 158.3, 157.3, 155.0, 149.4, 142.0, 135.7, 135.0, 132.3, 131.9, 129.4, 129.0, 125.19 (d, $J = 7.9$ Hz, 2C), 121.7, 120.7, 115.7, 115.6 (d, $J = 22.2$ Hz, 2C), 54.3, 41.3. HRMS: m/z 440.1177 [M+H]⁺. HRMS (ESI₊) m/z calcd for C₂₁H₁₉FN₅O₃S [M+H]⁺, 440.1187; found, 440.1177.

4.1.25.

N-(5-(4-((3-chloro-4-fluorophenyl)amino)quinazolin-6-yl)-2-methoxy-pyridin-3-yl)methanesulfonamide (**6c**)

61.2% yield, mp 257-259 °C. ¹H NMR (400 MHz, DMSO) δ 10.02 (s, 1H, NH), 9.45 (s, 1H, NH), 8.79 (s, 1H, Ar-H), 8.65 (s, 1H, Ar-H), 8.54 (d, $J = 2.2$ Hz, 1H, Ar-H), 8.21 - 8.17 (m, 2H, Ar-H), 8.10 (d, $J = 2.2$ Hz, 1H, Ar-H), 7.89 (d, $J = 8.7$ Hz, 1H, Ar-H), 7.85 (ddd, $J = 8.9, 4.2, 2.9$ Hz, 1H, Ar-H), 7.48 (t, $J = 9.1$ Hz, 1H, Ar-H), 4.02 (s, 3H, OCH₃), 3.12 (s, 3H, CH₃). ¹³C NMR (100 MHz, DMSO) δ 158.0, 157.3, 154.8, 154.0 (d, $J = 241.7$ Hz), 149.5, 142.0, 136.8 (d, $J = 2.6$ Hz), 135.2, 132.3, 132.1, 129.4, 129.1, 124.4, 123.2 (d, $J = 6.8$ Hz), 121.8, 120.6, 119.4 (d, $J = 18.3$ Hz), 117.1 (d, $J = 21.8$ Hz), 115.7, 54.3, 41.4. HRMS (ESI₊) m/z calcd for C₂₁H₁₈ClFN₅O₃S [M+H]⁺, 474.0797; found, 474.0799.

4.1.26. *N*-(5-(4-((2,4-difluorophenyl)amino)quinazolin-6-yl)-2-methoxy-pyridin-3-yl)methanesulfonamide (**6d**)

67.4% yield, mp 148-150 °C. ¹H NMR (400 MHz, DMSO) δ 10.00 (s, 1H, NH), 9.46 (s, 1H, NH), 8.79 (s, 1H, Ar-H), 8.61 - 8.48 (m, 2H, Ar-H), 8.22 (d, $J = 8.6$ Hz, 1H, Ar-H), 8.14 (s, 1H, Ar-H), 7.90 (d, $J = 8.7$ Hz, 1H, Ar-H), 7.63 (dd, $J = 15.0, 8.6$ Hz, 1H, Ar-H), 7.43 (dd, $J = 13.8, 5.6$ Hz, 1H, Ar-H), 7.20 (t, $J = 7.7$ Hz, 1H, Ar-H), 4.02 (s, 3H, OCH₃), 3.12 (s, 3H, CH₃). ¹³C NMR (150 MHz, DMSO) δ 160.6 (dd, $J = 11.6, 243.6$ Hz), 159.3, 157.6 (dd, $J = 8.6, 248.4$ Hz), 157.4, 155.3, 149.4, 142.0, 134.9, 132.5, 132.0, 130.2 (dd, $J = 2.1, 9.8$ Hz), 129.3, 129.0, 123.1 (dd, $J = 3.5, 12.5$ Hz), 121.7, 120.7, 115.4, 111.9 (dd, $J = 3.2, 21.9$ Hz), 105.2 (t, $J = 26.0$ Hz), 54.4, 41.3. HRMS (ESI₊) m/z calcd for C₂₁H₁₈F₂N₅O₃S [M+H]⁺, 458.1093; found, 458.1080.

N-(2-methoxy-5-(4-((4-(trifluoromethoxy)phenyl)amino)quinazolin-6-yl)pyridin-3-yl)methanesulfonamide (**6e**)

65.8% yield, mp 156-158 °C. ¹H NMR (400 MHz, DMSO) δ 10.06 (s, 1H, NH), 9.45 (s, 1H, NH), 8.82 (s, 1H, Ar-H), 8.63 (s, 1H, Ar-H), 8.55 (d, *J* = 2.1 Hz, 1H, Ar-H), 8.19 (d, *J* = 8.6 Hz, 1H, Ar-H), 8.11 (d, *J* = 2.1 Hz, 1H, Ar-H), 7.99 (d, *J* = 9.0 Hz, 2H, Ar-H), 7.90 (d, *J* = 8.6 Hz, 1H, Ar-H), 7.44 (d, *J* = 8.7 Hz, 2H, Ar-H), 4.02 (s, 3H, OCH₃), 3.12 (s, 3H, CH₃). ¹³C NMR (150 MHz, DMSO) δ 162.8, 158.1, 157.3, 154.9, 149.5, 142.0, 138.7, 135.1, 132.4, 132.1, 129.4, 129.1, 124.3(2C), 121.8(2C), 121.7, 120.7, 120.6(*q*, *J* = 169.3 Hz), 115.8, 54.3, 41.3. HRMS (ESI⁺) *m/z* calcd for C₂₂H₁₉F₃N₅O₄S [M+H]⁺, 506.1104; found, 506.1127.

4.1.28. *N*-(2-methoxy-5-(4-((4-methoxyphenyl)amino)quinazolin-6-yl)pyridin-3-yl)methanesulfonamide (**6f**)

54.9% yield, mp 141-143 °C. ¹H NMR (400 MHz, DMSO) δ 9.93 (s, 1H, NH), 9.45 (s, 1H, NH), 8.81 (s, 1H, Ar-H), 8.60 - 8.50 (m, 2H, Ar-H), 8.15 (d, *J* = 8.7 Hz, 1H, Ar-H), 8.11 (d, *J* = 2.0 Hz, 1H, Ar-H), 7.85 (d, *J* = 8.6 Hz, 1H, Ar-H), 7.69 (d, *J* = 8.9 Hz, 2H, Ar-H), 7.01 (d, *J* = 8.9 Hz, 2H, Ar-H), 4.01 (s, 3H, OCH₃), 3.79 (s, 3H, OCH₃), 3.12 (s, 3H, CH₃). ¹³C NMR (100 MHz, DMSO) δ 158.4, 157.3, 156.5, 155.2, 149.2, 142.0, 134.8, 132.4, 132.2, 131.8, 129.4, 128.8, 125.1, 121.7, 120.7, 115.8, 114.2, 55.7, 54.3, 41.3. HRMS (ESI⁺) *m/z* calcd for C₂₂H₂₂N₅O₄S [M+H]⁺, 452.1387; found, 452.1379.

4.1.29. *N*-(5-(4-((3,4-dimethoxyphenyl)amino)quinazolin-6-yl)-2-methoxypyridin-3-yl)methanesulfonamide (**6g**)

60.1% yield, mp 151-153 °C. ¹H NMR (400 MHz, DMSO) δ 9.90 (s, 1H, NH), 9.47 (s, 1H, NH), 8.84 (s, 1H, Ar-H), 8.57 (d, *J* = 2.1 Hz, 2H, Ar-H), 8.15 (d, *J* = 8.7 Hz, 1H, Ar-H), 8.12 (d, *J* = 2.1 Hz, 1H, Ar-H), 7.85 (d, *J* = 8.5 Hz, 1H, Ar-H), 7.46 (d, *J* = 1.9 Hz, 1H, Ar-H), 7.44 - 7.35 (m, 1H, Ar-H), 7.01 (d, *J* = 8.7 Hz, 1H, Ar-H), 4.02 (s, 3H, OCH₃), 3.81 (s, 3H, OCH₃), 3.79 (s, 3H, OCH₃), 3.12 (s, 3H, CH₃). ¹³C NMR (100 MHz, DMSO) δ 158.4, 157.3, 155.2, 149.5, 148.9, 146.1, 142.0, 134.8, 132.7, 132.4, 131.7, 129.5, 129.0, 121.8, 120.7, 115.9, 115.7, 112.2, 108.6, 56.2, 56.1, 54.3, 41.4. HRMS (ESI⁺) *m/z* calcd for C₂₃H₂₄N₅O₅S [M+H]⁺, 482.1493; found, 482.1488.

4.1.30.

N-(5-(4-((3-chloro-4-methoxyphenyl)amino)quinazolin-6-yl)-2-methoxypyridin-3-yl)methanesulfonamide (**6h**)

61.7% yield, mp 146-148 °C. ¹H NMR (400 MHz, DMSO) δ 9.90 (s, 1H, NH), 9.46 (s, 1H, NH), 8.78 (s, 1H, Ar-H), 8.67 - 8.51 (m, 2H, Ar-H), 8.16 (d, *J* = 8.5 Hz, 1H, Ar-H), 8.11 (d, *J* = 1.8 Hz, 1H, Ar-H), 8.00 (d, *J* = 2.1 Hz, 1H, Ar-H), 7.86 (d, *J* = 8.6 Hz, 1H, Ar-H), 7.76 (dd, *J* = 8.8, 2.1 Hz, 1H, Ar-H), 7.22 (d, *J* = 9.0 Hz, 1H, Ar-H), 4.02 (s, 3H, OCH₃), 3.89 (s, 3H, OCH₃), 3.13 (s, 3H, CH₃). ¹³C NMR (100 MHz,

DMSO) δ 158.1, 157.3, 155.0, 151.6, 149.4, 142.0, 134.9, 133.0, 132.3, 131.9, 129.4, 129.0, 124.7, 123.0, 121.7, 120.8, 120.6, 115.7, 113.1, 56.7, 54.3, 41.3. HRMS (ESI₊) m/z calcd for C₂₂H₂₁ClN₅O₄S [M+H]⁺, 486.0997; found, 486.0992.

4.1.31. methyl 3-((6-(6-methoxy-5-(methylsulfonamido)pyridin-3-yl)quinazolin-4-yl)amino)benzoate (6i)

58.4% yield, mp 240-242 °C. ¹H NMR (400 MHz, DMSO) δ 10.09 (s, 1H, NH), 9.46 (s, 1H, NH), 8.85 (s, 1H, Ar-H), 8.66 (s, 1H, Ar-H), 8.57 (s, 1H, Ar-H), 8.45 (s, 1H, Ar-H), 8.32 (d, J = 7.8 Hz, 1H, Ar-H), 8.19 (d, J = 8.6 Hz, 1H, Ar-H), 8.12 (s, 1H, Ar-H), 7.90 (d, J = 8.6 Hz, 1H, Ar-H), 7.75 (d, J = 7.6 Hz, 1H, Ar-H), 7.58 (t, J = 7.9 Hz, 1H, Ar-H), 4.02 (s, 3H, OCH₃), 3.90 (s, 3H, OCH₃), 3.13 (s, 3H, CH₃). ¹³C NMR (100 MHz, DMSO) δ 166.6, 158.1, 157.3, 154.9, 149.6, 142.0, 140.0, 135.2, 132.4, 132.1, 130.4, 129.4, 129.1, 127.3, 124.7, 123.1, 121.8, 120.7, 115.9, 54.3, 52.7, 41.3. HRMS (ESI₊) m/z calcd for C₂₃H₂₂N₅O₅S [M+H]⁺, 480.1336; found, 480.1323.

4.1.32. methyl

2-fluoro-5-((6-(6-methoxy-5-(methylsulfonamido)pyridin-3-yl)quinazolin-4-yl)amino)benzoate (6j)

63.6% yield, mp 246-248 °C. ¹H NMR (400 MHz, DMSO) δ 10.09 (s, 1H, NH), 9.45 (s, 1H, NH), 8.82 (s, 1H, Ar-H), 8.63 (s, 1H, Ar-H), 8.55 (d, J = 2.1 Hz, 1H, Ar-H), 8.34 (dd, J = 6.4, 2.7 Hz, 1H, Ar-H), 8.31 - 8.24 (m, 1H, Ar-H), 8.19 (d, J = 8.6 Hz, 1H, Ar-H), 8.10 (d, J = 2.1 Hz, 1H, Ar-H), 7.90 (d, J = 8.7 Hz, 1H, Ar-H), 7.48 - 7.39 (m, 1H, Ar-H), 4.02 (s, 3H, OCH₃), 3.90 (s, 3H, OCH₃), 3.12 (s, 3H, OCH₃). ¹³C NMR (100 MHz, DMSO) δ 164.4 (d, J = 3.7 Hz), 158.8, 157.6 (d, J = 253.4 Hz), 157.3, 154.9, 149.5, 142.0, 135.9 (d, J = 2.9 Hz), 135.2, 132.2, 132.1, 129.4, 129.3 (d, J = 8.4 Hz), 129.1, 125.3, 121.8, 120.7, 118.2 (d, J = 11.2 Hz), 117.6 (d, J = 23.3 Hz), 115.7, 54.3, 52.9, 41.4. HRMS (ESI₊) m/z calcd for C₂₃H₂₁FN₅O₅S [M+H]⁺, 498.1242; found, 498.1245.

4.1.33. methyl

2-chloro-5-((6-(6-methoxy-5-(methylsulfonamido)pyridin-3-yl)quinazolin-4-yl)amino)benzoate (6k)

49.7% yield, mp 247-249 °C. ¹H NMR (400 MHz, DMSO) δ 10.11 (s, 1H, NH), 9.46 (s, 1H, NH), 8.82 (s, 1H, Ar-H), 8.67 (s, 1H, Ar-H), 8.55 (d, J = 1.6 Hz, 1H, Ar-H), 8.35 (d, J = 2.2 Hz, 1H, Ar-H), 8.26 (dd, J = 8.8, 2.3 Hz, 1H, Ar-H), 8.19 (d, J = 8.5 Hz, 1H, Ar-H), 8.10 (d, J = 1.6 Hz, 1H, Ar-H), 7.90 (d, J = 8.6 Hz, 1H, Ar-H), 7.63 (d, J = 8.8 Hz, 1H, Ar-H), 4.02 (s, 3H, OCH₃), 3.91 (s, 3H, OCH₃), 3.12 (s, 3H, CH₃). ¹³C NMR (100 MHz, DMSO) δ 165.8, 157.9, 157.3, 154.7, 149.6, 142.0, 138.8, 135.3, 132.3, 132.2, 131.4, 130.1, 129.4, 129.2, 126.8, 126.3, 124.5, 121.8, 120.7, 115.8, 54.4, 53.1, 41.4. HRMS (ESI₊) m/z calcd for C₂₃H₂₁ClN₅O₅S [M+H]⁺, 514.0946; found, 514.0947.

4.1.34. methyl

(6l)

48.5% yield, mp 155-157 °C. ¹H NMR (400 MHz, DMSO) δ 10.07 (s, 1H, NH), 9.47 (s, 1H, NH), 8.84 (s, 1H, Ar-H), 8.73 (s, 1H, Ar-H), 8.57 (s, 1H, Ar-H), 8.20 (d, *J* = 8.7 Hz, 1H, Ar-H), 8.11 (s, 1H, Ar-H), 7.93 (d, *J* = 8.7 Hz, 1H, Ar-H), 7.84 (s, 1H, Ar-H), 7.79 (d, *J* = 8.5 Hz, 1H, Ar-H), 7.72 (d, *J* = 8.5 Hz, 1H, Ar-H), 4.02 (s, 3H, OCH₃), 3.89 (s, 3H, OCH₃), 3.79 (s, 3H, OCH₃), 3.12 (s, 3H, CH₃). ¹³C NMR (100 MHz, DMSO) δ 166.0, 159.8, 158.0, 157.3, 154.7, 149.7, 144.9, 142.1, 135.3, 132.4, 132.3, 132.2, 129.4, 129.2, 121.8, 120.8, 116.0, 114.4, 113.4, 105.8, 56.3, 54.3, 52.1, 41.4. HRMS (ESI₊) *m/z* calcd for C₂₄H₂₄N₅O₆S [M+H]⁺, 510.1442; found, 510.1417.

4.1.35.

N-(5-(4-((3-chloro-4-((4-fluorobenzyl)oxy)phenyl)amino)quinazolin-6-yl)-2-methoxy)pyridin-3-yl)methanesulfonamide (**6m**)

60.9% yield, mp 168-170 °C. ¹H NMR (400 MHz, DMSO) δ 9.91 (s, 1H, NH), 9.45 (s, 1H, NH), 8.78 (s, 1H, Ar-H), 8.60 (s, 1H, Ar-H), 8.54 (s, 1H, Ar-H), 8.17 (d, *J* = 8.7 Hz, 1H, Ar-H), 8.10 (d, *J* = 1.7 Hz, 1H, Ar-H), 8.01 (d, *J* = 1.9 Hz, 1H, Ar-H), 7.87 (d, *J* = 8.7 Hz, 1H, Ar-H), 7.74 (dd, *J* = 8.9, 2.0 Hz, 1H, Ar-H), 7.56 (d, *J* = 6.0 Hz, 1H, Ar-H), 7.54 (d, *J* = 5.7 Hz, 1H, Ar-H), 7.32 - 7.24 (m, 3H, Ar-H), 5.22 (s, 2H, CH₂), 4.01 (s, 3H, OCH₃), 3.11 (s, 3H, CH₃). ¹³C NMR (100 MHz, DMSO) δ 162.3 (d, *J* = 242.0 Hz), 158.1, 157.3, 155.0, 150.4, 149.6, 142.0, 135.0, 133.4, 133.3, 132.3, 131.9, 130.3 (d, *J* = 8.4 Hz, 2C), 129.4, 129.1, 124.7, 122.9, 121.8, 121.6, 120.6, 115.8 (d, *J* = 21.3 Hz, 2C), 115.7, 114.9, 70.1, 54.3, 41.3. HRMS (ESI₊) *m/z* calcd for C₂₈H₂₄ClFN₅O₄S [M+H]⁺, 580.1216; found, 580.1222.

4.1.36.

N-(5-(4-((3-chloro-4-fluorophenyl)amino)quinazolin-6-yl)-2-methoxy)pyridin-3-yl)butane-1-sulfonamide (**6n**)

65.8% yield, mp 255-257 °C. ¹H NMR (400 MHz, DMSO) δ 10.02 (s, 1H, NH), 9.51 (s, 1H, NH), 8.80 (s, 1H, Ar-H), 8.68 (s, 1H, Ar-H), 8.56 (d, *J* = 1.8 Hz, 1H, Ar-H), 8.22 (d, *J* = 2.3 Hz, 1H, Ar-H), 8.19 (d, *J* = 9.2 Hz, 1H, Ar-H), 8.14 (d, *J* = 1.9 Hz, 1H, Ar-H), 7.91 (d, *J* = 8.7 Hz, 1H, Ar-H), 7.90 - 7.83 (m, 1H, Ar-H), 7.50 (t, *J* = 9.1 Hz, 1H, Ar-H), 4.04 (s, 3H, OCH₃), 3.26 - 3.15 (m, 2H, CH₂), 1.79 (dt, *J* = 15.2, 7.7 Hz, 2H, CH₂), 1.53 - 1.36 (m, 2H, CH₂), 0.93 (t, *J* = 7.3 Hz, 3H, CH₃). ¹³C NMR (100 MHz, DMSO) δ 158.0, 157.3, 154.8, 153.9 (d, *J* = 241.9 Hz), 149.5, 142.0, 136.8 (d, *J* = 2.8 Hz), 135.1, 132.7, 132.1, 129.3, 129.1, 124.3, 123.1 (d, *J* = 6.5 Hz), 121.7, 120.6, 119.4 (d, *J* = 18.5 Hz), 117.1 (d, *J* = 21.8 Hz), 115.7, 54.3, 52.6, 25.7, 21.3, 14.0. HRMS (ESI₊) *m/z* calcd for C₂₄H₂₄ClFN₅O₃S [M+H]⁺, 516.1267; found, 516.1283.

4.1.37. ethyl 3-((6-(5-(butylsulfonamido)-6-methoxy)pyridin-3-yl)quinazolin-4-yl)amino)benzoate (**6o**)

67.0% yield, mp 116-118 °C. ¹H NMR (400 MHz, DMSO) δ 10.11 (s, 1H, NH), 9.48 (s, 1H, NH), 8.86 (s, 1H, Ar-H), 8.65 (s, 1H, Ar-H), 8.56 (s, 1H, Ar-H), 8.42 (s, 1H, Ar-H), 8.33 (d, *J* = 5.6 Hz, 1H, Ar-H), 8.18 (d, *J* = 7.5 Hz, 1H, Ar-H), 8.13 (s, 1H, Ar-H), 7.90 (d, *J* = 6.9 Hz, 1H, Ar-H), 7.75 (d, *J* = 5.4 Hz, 1H, Ar-H), 7.58 (s, 1H, Ar-H), 4.37 (d, *J* = 5.2 Hz, 2H, CH₂), 4.02 (s, 3H, OCH₃), 3.17 (s, 2H, CH₂), 1.77 (s, 2H, CH₂), 1.41 (s, 2H, CH₂), 1.36 (s, 3H, CH₃), 0.90 (s, 3H, CH₃). ¹³C NMR (100 MHz, DMSO) δ 166.1, 158.1, 157.3, 154.9, 149.6, 142.1, 134.0, 135.1, 132.7, 132.0, 130.7, 129.4, 129.3, 129.1, 127.3, 124.7, 123.1, 121.7, 120.7, 115.9, 61.3, 54.3, 52.6, 25.7, 21.3, 14.7, 14.0. HRMS (ESI₊) *m/z* calcd for C₂₇H₃₀N₅O₅S [M+H]⁺, 536.1962; found, 536.1966.

4.1.38. methyl

3-((6-(5-(2,4-difluorophenylsulfonamido)-6-methoxy-pyridin-3-yl)quinazolin-4-yl)amino)benzoate (**6p**)

66.1% yield, mp 244-246 °C. ¹H NMR (400 MHz, DMSO) δ 10.40 (s, 1H, NH), 10.09 (s, 1H, NH), 8.85 (s, 1H, Ar-H), 8.66 (s, 1H, Ar-H), 8.58 (d, *J* = 2.2 Hz, 1H, Ar-H), 8.46 (s, 1H, Ar-H), 8.33 (d, *J* = 8.1 Hz, 1H, Ar-H), 8.20 (dd, *J* = 0.8, 9.2 Hz, 1H, Ar-H), 8.18 (s, 1H, Ar-H), 7.90 (d, *J* = 8.7 Hz, 1H, Ar-H), 7.80 - 7.74 (m, 2H, Ar-H), 7.63 - 7.57 (m, 2H, Ar-H), 7.21 (td, *J* = 8.6, 1.9 Hz, 1H, Ar-H), 3.91 (s, 3H, OCH₃), 3.66 (s, 3H, OCH₃). ¹³C NMR (150 MHz, DMSO) δ 166.6, 165.5 (dd, *J* = 12.0, 253.1 Hz), 162.8, 159.9 (dd, *J* = 13.1, 255.9 Hz), 158.5, 158.1, 154.9, 149.6, 143.6, 140.0, 135.6, 134.7, 132.3 (d, *J* = 16.1 Hz), 131.9, 130.4, 129.5, 129.3, 129.2, 127.7, 125.6 (dd, *J* = 3.0, 21.5 Hz), 124.7, 123.1, 120.7, 120.0, 115.9, 112.2 (d, *J* = 33.2 Hz), 106.2 (t, *J* = 38.9 Hz), 53.9, 52.7. HRMS (ESI₊) *m/z* calcd for C₂₂H₂₂F₂N₅O₅S [M+H]⁺, 578.1304; found, 578.1310.

4.1.39. N-(5-(4-((6-fluoropyridin-3-yl)amino)quinazolin-6-yl)-2-methoxy-pyridin-3-yl)methanesulfonamide (**6q**)

63.7% yield, mp 172-174 °C. ¹H NMR (400 MHz, DMSO) δ 10.13 (s, 1H, NH), 9.46 (s, 1H, NH), 8.79 (s, 1H, Ar-H), 8.64 (s, 1H, Ar-H), 8.62 (s, 1H, Ar-H), 8.54 (d, *J* = 1.9 Hz, 1H, Ar-H), 8.45 (dd, *J* = 11.1, 4.7 Hz, 1H, Ar-H), 8.20 (d, *J* = 8.5 Hz, 1H, Ar-H), 8.10 (d, *J* = 1.9 Hz, 1H, Ar-H), 7.90 (d, *J* = 8.6 Hz, 1H, Ar-H), 7.28 (dd, *J* = 8.7, 2.9 Hz, 1H, Ar-H), 4.02 (s, 3H, OCH₃), 3.12 (s, 3H, CH₃). ¹³C NMR (101 MHz, DMSO) δ 159.5 (d, *J* = 241.7 Hz), 158.3, 157.3, 154.9, 149.5, 142.0, 141.6 (d, *J* = 15.6 Hz), 136.9 (d, *J* = 8.1 Hz), 135.2, 134.5 (d, *J* = 4.1 Hz), 132.3, 132.2, 129.3, 129.1, 121.8, 120.7, 115.7, 109.5 (d, *J* = 39.1 Hz), 54.4, 41.3. HRMS (ESI₊) *m/z* calcd for C₂₀H₁₈FN₆O₃S [M+H]⁺, 441.1140; found, 441.1145.

4.1.40. N-(2-methoxy-5-(4-((6-methoxy-pyridin-3-yl)amino)quinazolin-6-yl)pyridin-3-yl)methanesulfonamide (**6r**)

63.7% yield, mp 143-145 °C. ¹H NMR (400 MHz, DMSO) δ 10.00 (s, 1H, NH), 9.47 (s, 1H, NH), 8.78 (s, 1H, Ar-H), 8.55 (s, 2H, Ar-H), 8.51 (s, 1H, Ar-H), 8.17 (d, *J* = 8.6 Hz, 1H, Ar-H), 8.10 (d, *J* = 7.6 Hz, 2H, Ar-H), 7.86 (d, *J* = 8.6 Hz, 1H, Ar-H), 6.92 (d, *J* = 8.8 Hz, 1H, Ar-H), 4.02 (s, 3H, OCH₃), 3.89 (s, 3H,

OCH₃), 3.12 (s, 3H, CH₃). ¹³C NMR (100 MHz, DMSO) δ 160.8, 158.7, 157.3, 155.1, 149.4, 142.0, 141.8, 135.8, 134.9, 132.4, 131.9, 130.1, 129.4, 129.0, 121.7, 120.7, 115.7, 110.4, 54.3, 53.7, 41.3. HRMS (ESI⁺) *m/z* calcd for C₂₁H₂₁N₆O₄S [M+H]⁺, 453.1340; found, 453.1355.

4.2. Biological assay methods

4.2.1. Cell culture

A549, BT549, HCT-116, MCF-7, SK-HEP-1 and SNU638 cells were purchased from the American Type Culture Collection (Manassas, VA, USA). Cells were grown in DMEM (SNU-638, BT549, MCF-7 and SK-HEP-1) or RPMI1640 (HCT-116 and A549 cells) supplemented with 10% FBS and antibiotics-antimycotics (PSF; 100 units/mL penicillin G sodium, 100 µg/mL streptomycin and 250 ng/mL amphotericin B) in a humidified incubator containing 5% CO₂ at 37 °C.

4.2.2. Antiproliferative activity

The cell viability was evaluated using the sulforhodamine B (SRB) cellular protein-staining method with minor modifications. Briefly, cells were treated with various concentrations of compounds in 96-well plates and incubated at 37 °C in a humidified atmosphere with 5% CO₂ for 72 h. After treatment, the cells were fixed with 10% TCA solution, and cell viability was determined with SRB assay. The percentage of cell-growth inhibition was calculated using the formulae below. The IC₅₀ values were calculated using a non-linear regression analysis (percent growth versus concentration). Percent growth inhibition = 100 - 100 × (OD_{sample} - OD_{Day0}) / (OD_{neg control} - OD_{Day0}).

4.2.3. EGFR and PI3K enzymatic activity assay

A mobility shift assay was used to measure the potency of title compounds against EGFR. The kinase base buffer was consist of 50 mM HEPES (pH 7.5), 10 mM MgCl₂, 2 mM DTT and 0.0015% Brij35, while the stop buffer contained a mixture of 100 mM HEPES (pH 7.5), 50 mM EDTA, 0.015% Brij-35 and 0.2% Coating Reagent #3. Dilute the tested compounds to 50-fold of the final desired highest inhibitor concentration in reaction by 100% DMSO. Subsequently, dilute the compounds by transferring 30 µL to 60 µL of 100% DMSO in the next well and so forth for a total of 10 concentrations. Add 100 µL of 100% DMSO to two empty wells for no compound control and no enzyme control in the same 96-well plate. Mark the plate as source plate. Transfer 10 µL of compound from source plate to a new 96-well plate as the intermediate plate. Add 90 µL of 1-fold kinase buffer to each well of the intermediate plate. Mix the compound in intermediate plate for 10 min on the shaker. The assay plate was prepared after transferring 5 µL of each well from the 96-well intermediate plate to a 384-well plate in duplicates. The prepared enzyme solution was added to the assay plate, which was then incubated at room temperature for 10 min, followed by the addition 10 µL of 2.5-fold peptide solution (FAM-labeled peptide and ATP in kinase base buffer). The mixture was incubated at 28 °C for another 1 h, then add 25 µL of stop buffer to stop the reaction. The

conversion data was copied from Caliper program, and the values were converted to inhibition values.

Percent inhibition = $(\text{max} - \text{conversion}) / (\text{max} - \text{min}) \times 100$. Fit the data in XLFit excel add-in version 4.3.1 to obtain IC₅₀ values. Equation used is: $Y = \text{Bottom} + (\text{Top} - \text{Bottom}) / (1 + (\text{IC}_{50}/X)^{\text{Hillslope}})$

The PI3K kinase assay was measured by PI3 Kinase Activity/Inhibitor Assay Kit (EMD Millipore, #17-493) following the manufacturer's protocols.

4.2.4. Colony formation assay

BT549 cells were seeded in a 6-well plates with a density of 3×10^3 cells/well and then were cultured with different concentrations (0, 1.0, 2.5, 5.0 μM) of **6c** about 2 weeks. Cells were fixed by ethanol and stained with crystal violet.

4.2.5. Annexin V-FITC and propidium iodide (PI) double staining assay

BT549 cells were seeded in a 6-well plates (2×10^5 cells/well) and treated with **6c** mentioned above. At the end of treatments, the cells were harvested and washed by cold PBS. Then the resuspended cells (1×10^6) were incubated with Annexin VFITC (5 μL) and PI (5 μL) at room temperature for 5 min in the dark and examined with flow cytometry.

4.2.6. DAPI staining assay

Apoptotic feature of BT549 cells was assessed by DNA condensation using DAPI (4',6-diamidino-2-phenylindole). 2×10^4 BT549 cells were seeded in a 6-well plates and incubated with **6c** for 24 h. Then, cells were stained with DAPI for 10 min and observed under a fluorescence microscope.

4.2.7. Cell cycle analysis

Cell cycle was determined by the staining of DNA with propidium iodide (PI). 2×10^5 BT549 cells were incubated with **6c** for 24 h and fixed in 70% ethanol overnight. Then, cells were washed with PBS and treated with RNase and PI for 1 h. The percentages of cells in different phase of cell cycle were measured by flow cytometer.

4.2.8. Western blot analysis

Total cell lysates were prepared in RIPA buffer (50 mM Tris-HCl, pH 8.0, 150 mM NaCl, 1% NP-40, 0.5% sodium deoxycholate, 0.1% SDS). The protein concentration was determined, and equal amounts of protein samples were subjected to 10% SDS-PAGE followed by transferring to PVDF membranes, and probed with were subsequently analyzed with EGFR, p-EGFR, AKT and p-AKT antibodies. Exposures were obtained using ImageQuant LAS 4000 biomolecular imager (GE Healthcare).

4.2.9. Molecular docking studies

The crystal structure of EGFR (PDB entry code: 4WKQ) in complex with Gefitinib and the PI3K (PDB entry code: 3L08) in complex with Omipalisib were used for molecular modeling. The AutoDock 4.2 was used to perform docking calculations. Polar hydrogens and partial charges were added by Sybyl 6.9.1, and

energy minimization was made employing both steepest descent and conjugate gradients protocols. The optimized AutoDocking parameters are as follows: the maximum number of energy evaluations was increased to 25,000,000 per run; the iterations of Solis & Wets local search was 3000; the number of individuals in population was 300 and the number of generations was 100. Accelrys Discovery Studio Visualizer 4.0 was used for graphic display.

Acknowledgments

Financial supported by Career Development Support Plan for Young and Middle-aged Teachers in Shenyang Pharmaceutical University (Grant No. ZQN2015023) is gratefully acknowledged.

References

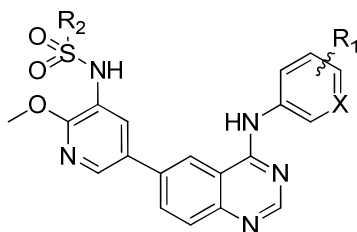
- [1] X. Wu, M. Li, Y. Qu, W. Tang, Y. Zheng, J. Lian, M. Ji, L. Xu, Design and synthesis of novel Gefitinib analogues with improved anti-tumor activity, *Bioorganic & Medicinal Chemistry*, 18 (2010) 3812-3822.
- [2] H.Q. Zhang, F.H. Gong, J.Q. Ye, C. Zhang, X.H. Yue, C.G. Li, Y.G. Xu, L.P. Sun, Design and discovery of 4-anilinoquinazoline-urea derivatives as dual TK inhibitors of EGFR and VEGFR-2, *European Journal of Medicinal Chemistry*, 125 (2017) 245-254.
- [3] Y. Yarden, M. X. Sliwkowski, Untangling the ErbB signalling network, *Nature Reviews Molecular Cell Biology*. 2 (2001) 127-137.
- [4] J. Marshall, Clinical implications of the mechanism of epidermal growth factor receptor inhibitors, *Cancer*, 107 (2006) 1207-1218.
- [5] M. Scaltriti, J. Baselga, The epidermal growth factor receptor pathway: a model for targeted therapy, *Clinical Cancer Research An Official Journal of the American Association for Cancer Research*, 12 (2006) 5268-5272.
- [6] M.M. Moasser, A. Basso, S.D. Averbuch, N. Rosen, The tyrosine kinase inhibitor ZD1839 ("Iressa") inhibits HER2-driven signaling and suppresses the growth of HER2-overexpressing tumor cells, *Cancer Research*, 61 (2001) 7184-7188.
- [7] S.R. Johnston, A. Leary, Lapatinib: a novel EGFR/HER2 tyrosine kinase inhibitor for cancer, *Drugs of Today*, 42 (2006) 441-453.
- [8] M.H. Cohen, J.R. Johnson, Y.F. Chen, R. Sridhara, R. Pazdur, FDA drug approval summary: erlotinib (Tarceva) tablets, *Oncologist*, 10 (2005) 461-466.
- [9] F. Carlomagno, D. Vitagliano, T. Guida, F. Ciardiello, G. Tortora, ZD6474, an Orally Available Inhibitor of KDR Tyrosine Kinase Activity, Efficiently Blocks Oncogenic RET Kinases, *Cancer Research*, 62 (2002) 7284-7290.
- [10] N. Minkovsky, A. Berezov, BIBW-2992, a dual receptor tyrosine kinase inhibitor for the treatment of solid tumors, *Current Opinion in Investigational Drugs*, 9 (2008) 1336-1346.

- [11] F. Tan, X. Shen, D. Wang, G. Xie, X. Zhang, L. Ding, Y. Hu, W. He, Y. Wang, Y. Wang, Icotinib (BPI-2009H), a novel EGFR tyrosine kinase inhibitor, displays potent efficacy in preclinical studies, *Lung Cancer*, 76 (2012) 177-182.
- [12] J.A. Engelman, L. Ji, L.C. Cantley, The evolution of phosphatidylinositol 3-kinases as regulators of growth and metabolism, *Nature Reviews Genetics*, 7 (2006) 606-619.
- [13] S.J. Leever, B. Vanhaesebroeck, M.D. Waterfield, Signalling through phosphoinositide 3-kinases: the lipids take centre stage, *Current Opinion in Cell Biology*, 11 (1999) 219-225.
- [14] P. Liu, H. Cheng, T.M. Roberts, J.J. Zhao, Targeting the phosphoinositide 3-kinase pathway in cancer, *Nature Reviews Drug Discovery*, 8 (2009) 627-644.
- [15] S. Volinia, I. Hiles, E. Ormondroyd, D. Nizetic, R. Antonacci, M. Rocchi, M.O. Waterfield, Molecular Cloning, cDNA Sequence, and Chromosomal Localization of the Human Phosphatidylinositol 3-Kinase p110 α (PIK3CA) Gene, *Genomics*, 24 (1994) 472-477.
- [16] V. Asati, D.K. Mahapatra, S.K. Bharti, PI3K/Akt/mTOR and Ras/Raf/MEK/ERK signaling pathways inhibitors as anticancer agents: Structural and pharmacological perspectives, *European Journal of Medicinal Chemistry*, 109 (2016) 314-341.
- [17] C.D. Britten, PI3K and MEK inhibitor combinations: examining the evidence in selected tumor types, *Cancer Chemotherapy & Pharmacology*, 71 (2013) 1395-1409.
- [18] S.D. Knight, N.D. Adams, J.L. Burgess, A.M. Chaudhari, M.G. Darcy, C.A. Donatelli, J.I. Luengo, K.A. Newlander, C.A. Parrish, L.H. Ridgers, Discovery of GSK2126458, a Highly Potent Inhibitor of PI3K and the Mammalian Target of Rapamycin, *Acs Med Chem Lett*, 1 (2010) 39-43.
- [19] S. Maira, F. Stauffer, J. P. Furet, C. Schnell, C. Fritsch, S. Brachmann, P. Chene, A. De-Pover, K. Schoemaker, D. Fabbro, Identification and characterization of NVP-BEZ235, a new orally available dual phosphatidylinositol 3-kinase/mammalian target of rapamycin inhibitor with potent in vivo antitumor activity, *Molecular Cancer Therapeutics*, 7 (2008) 1851-1863.
- [20] L. Xi, J.Q. Zhang, Z.C. Liu, J.H. Zhang, J.F. Yan, Y. Jin, J. Lin, Novel 5-anilinoquinazoline-8-nitro derivatives as inhibitors of VEGFR-2 tyrosine kinase: synthesis, biological evaluation and molecular docking, *Organic & Biomolecular Chemistry*, 11 (2013) 4367-4378.
- [21] R.R. Yadav, S.K. Guru, P. Joshi, G. Mahajan, M.J. Mintoo, V. Kumar, S.S. Bharate, D.M. Mondhe, R.A. Vishwakarma, S. Bhushan, 6-Aryl substituted 4-(4-cyanomethyl) phenylamino quinazolines as a new class of isoform-selective PI3K- α inhibitors, *European Journal of Medicinal Chemistry*, 122 (2016) 731-743.
- [22] M. Xin, Y.Y. Hei, H. Zhang, Y. Shen, S.Q. Zhang, Design and synthesis of novel 6-aryl substituted 4-anilinequinazoline derivatives as potential PI3K δ inhibitors, *Bioorganic & Medicinal Chemistry Letters*, 27 (2017) 1972-1977.
- [23] K. Hoegenauer, N. Soldermann, F. Stauffer, P. Furet, N. Graveleau, A.B. Smith, C. Hebach, G.J. Hollingworth, I. Lewis, S. Gutmann, Discovery and Pharmacological Characterization of Novel Quinazoline-Based PI3K Delta-Selective Inhibitors,

[24] Y. Yosaatmadja, C.J. Squire, M. Mckeage, J.U. Flanagan, 1.85 angstrom structure of EGFR kinase domain with gefitinib.

ACCEPTED MANUSCRIPT

Table(s)

Table 1 Cytotoxicity *in vitro* of target compounds against five cancer cell lines (IC₅₀ Values^a in μ M).

Cells				A549	BT549	HCT-116	MCF-7	SK-HEP-1	SNU638
Comp.	R ₁	R ₂	X						
6a	3-F	✓	CH	9.94±0.23	2.76±0.07	3.94±0.08	8.02±0.26	1.85±0.06	2.76±0.08
6b	4-F	✓	CH	7.62±0.27	3.12±0.09	3.16±0.09	6.51±0.11	1.47±0.07	2.40±0.09
6c	3-Cl-4-F	✓	CH	8.23±0.34	1.02±0.08	5.60±0.24	5.59±0.21	6.10±0.26	4.10±0.13
6d	2,4-diF	✓	CH	4.71±0.17	2.48±0.14	4.01±0.15	1.61±0.07	2.49±0.12	2.05±0.08
6e	4-OCF ₃	✓	CH	25.36±0.51	8.24±0.16	16.59±0.25	23.68±0.38	6.14±0.31	22.4±0.21
6f	4-OCH ₃	✓	CH	3.58±0.16	1.88±0.10	3.49±0.09	1.79±0.09	1.61±0.06	3.97±0.15
6g	3,4-diOCH ₃	✓	CH	5.82±0.34	2.59±0.22	4.36±0.22	2.43±0.15	2.84±0.15	1.68±0.06
6h	3-Cl-4-OCH ₃	✓	CH	5.24±0.33	2.47±0.14	5.62±0.22	3.32±0.12	2.81±0.17	3.62±0.10
6i	3-COOCH ₃	✓	CH	1.10±0.05	1.08±0.09	0.40±0.02	10.1±0.09	2.40±0.09	1.12±0.03
6j	3-COOCH ₃ -4-F	✓	CH	3.42±0.13	2.74±0.25	2.36±0.12	1.15±0.09	5.18±0.16	2.54±0.08
6k	3-COOCH ₃ -4-Cl	✓	CH	2.13±0.07	2.36±0.21	3.13±0.19	1.43±0.11	7.06±0.32	2.20±0.12
6l	3-OCH ₃ -4-COOCH ₃	✓	CH	3.35±0.08	3.76±0.11	1.69±0.16	10.94±0.14	0.83±0.03	3.44±0.16
6m	3-Cl-4-(4-fluorobenzyl)oxy	✓	CH	31.3±0.44	14.6±0.23	5.41±0.31	28.36±0.54	1.95±0.07	2.36±0.14
6n	3-Cl-4-F	✓	CH	77.1±2.23	56.8±1.13	9.99±0.87	65.8±1.82	53.8±0.43	5.35±0.21
6o	3-COOCH ₂ C ₆ H ₄ H ₃	✓	CH	42.3±1.26	37.2±0.97	26.7±0.45	36.4±0.68	21.6±0.34	25.2±0.44

6p	3-COOCH ₃		CH	10.51±0.08	12.7±0.20	1.50±0.06	22.38±0.17	2.80±0.04	0.4±0.02
6q	6-F		N	6.72±0.21	4.78±0.16	7.62±0.34	5.39±0.22	5.24±0.17	6.52±0.26
6r	6-OCH ₃		N	5.56±0.23	3.49±0.18	6.91±0.23	3.77±0.13	3.44±0.11	4.28±0.18
Gefitini				8.27±0.42	6.56±0.35	5.98±0.72	26.7±1.02	10.1±0.32	7.56±0.24
b									
Dactolis				0.62±0.07	0.74±0.08	0.84±0.12	1.33±0.14	1.82±0.23	1.24±0.13
ib									

^aIC₅₀ values are the mean of triplicate measurements.

Table 2 Activities of **6c**, **6i** and Gefitinib, Dactolisib against EGFR and Class I PI3K (IC₅₀ Values in nM)

	EGFR	PI3K α	PI3K β	PI3K γ	PI3K δ
6c	2.4	317	9412	3560	8672
6i	409	165	4936	1783	4364
Gefitinib	2.3	ND	ND	ND	ND
Dactolisib	ND	16.4	35.9	23.6	78.4

ND: Not determined

Figure legends

Fig.1. The structures of some EGFR inhibitors.

Fig.2. The design strategy based on Dactolisib, Gefitinib and Omipalisib

Fig.3. The colony formation assay of compound **6c**. (A) treatment with compound **6c**, representative photographs of colony formation are shown. (B) Bar graphs showed the quantitative results of clonogenicity. Data are presented as the mean for three independent experiments. ** $P < 0.01$, *** $P < 0.001$ compared with control.

Fig.4. Apoptosis and the effect of compound **6c** on cell cycle. (A) AV-PI staining show early and late apoptosis of BT549 cells induced by compound **6c**. (B) Quantification of early and late apoptosis. (C) Hoechst 33342 staining and compound **6c** induced morphological changes. (D) Cell cycle changes after compound **6c** treatment. (E) Quantification of the percentages of cells in different phase.

Fig.5. Western blot analysis of **6c**. (A) The inhibition effects of compound **6c** (0.1 μM , 0.5 μM and 2.5 μM) on the expression of p-EGFR, EGFR in BT549 cells are depicted. β -Actin was used as internal control. (B) The inhibition effects of compound **6c** (5 μM , 10 μM and 20 μM) on the expression of p-Akt, Akt in BT549 cells are depicted. β -Actin was used as internal control.

Fig.6. Docking mode of **6c** with protein crystal structure of EGFR and PI3K. (A) Key interactions of compound **6c** in the active site of EGFR (PDB: 4WKQ). (B) The binding pose of **6c** and Gefitinib in the active site of EGFR. Gefitinib was highlighted with yellow. (C) Key interactions of compound **6c** in the active site of PI3K (PDB: 3L08). (D) The binding pose of **6c** and Omipalisib in the active site of PI3K. Omipalisib was highlighted with yellow.

Scheme 1. (a) benzenesulfonyl chloride, pyridine, rt, 24 h; (b) bis(pinacolato)diborane, Pd(dppf)₂Cl₂, AcOK, DMF, 100 °C, 8 h; (c) amines, isopropanol, 90 °C, 4h; (d) Pd(dppf)₂Cl₂, Cs₂CO₃, DMF/ H₂O, 90 °C, 8 h.

Figure 1

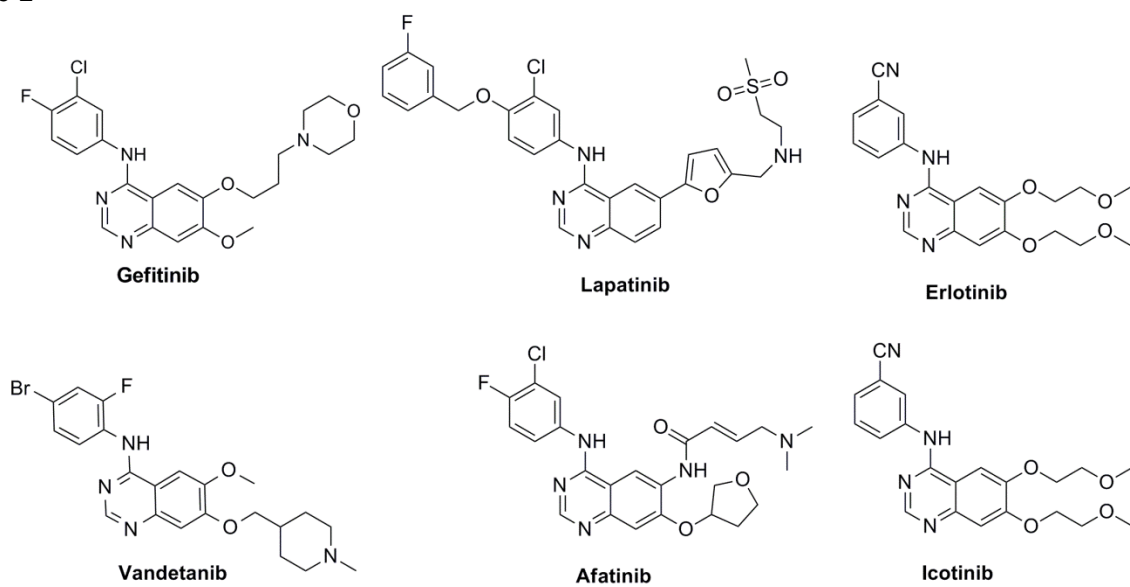


Figure 2

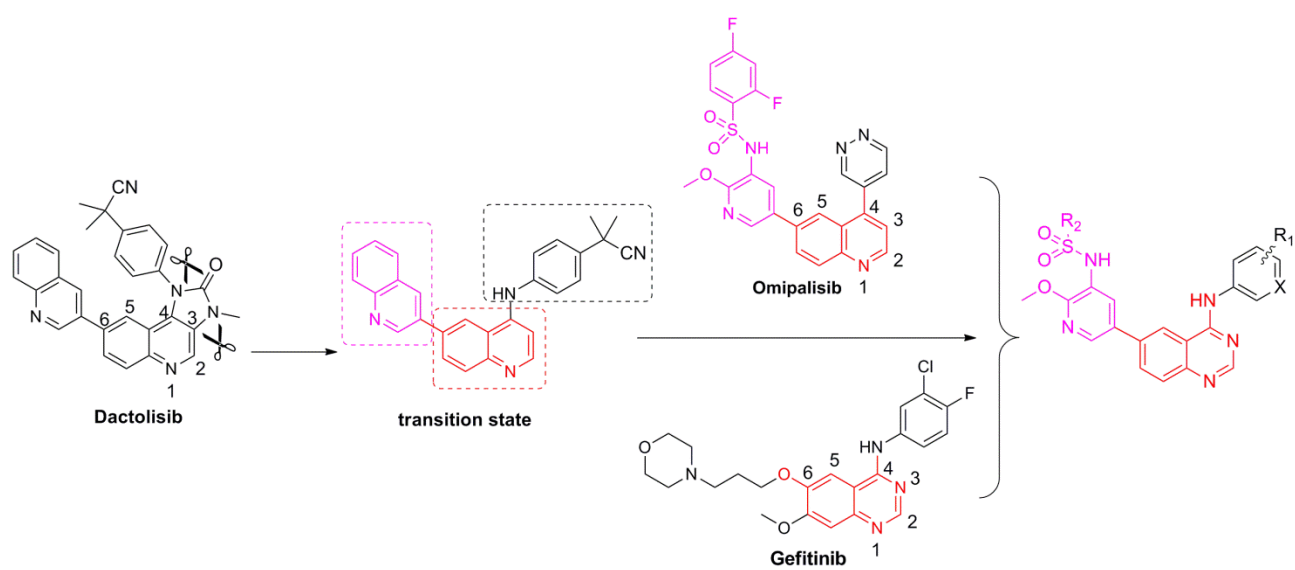


Figure 3

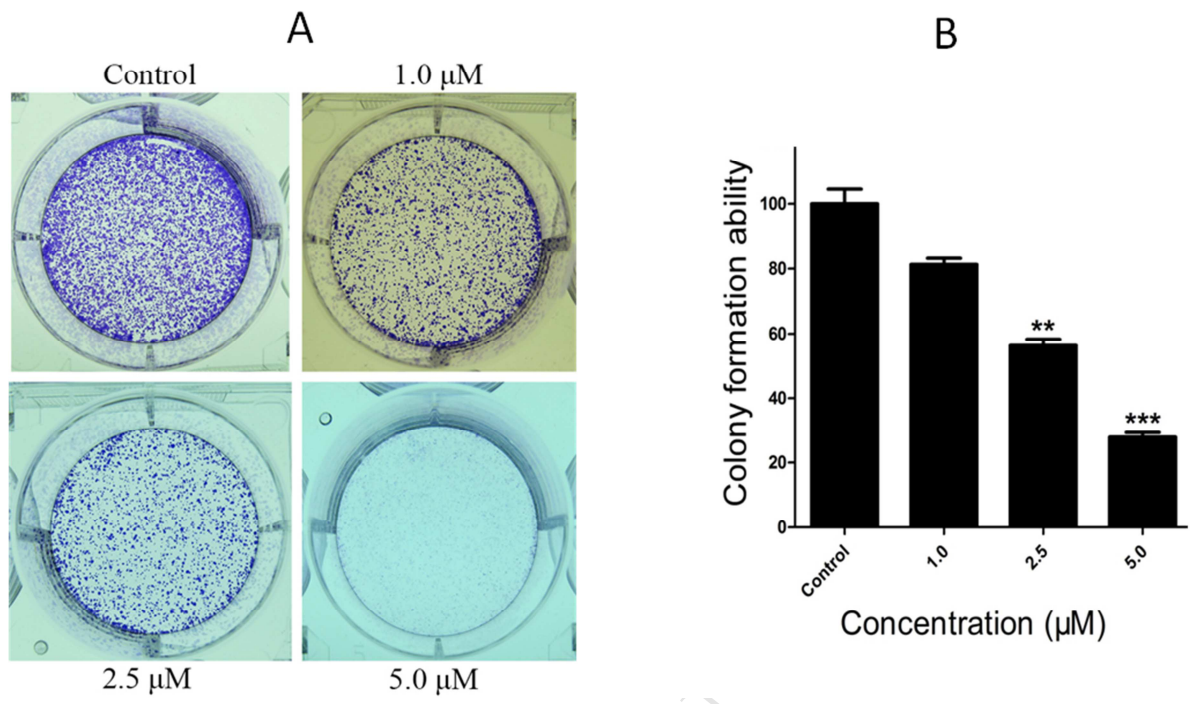


Figure 4

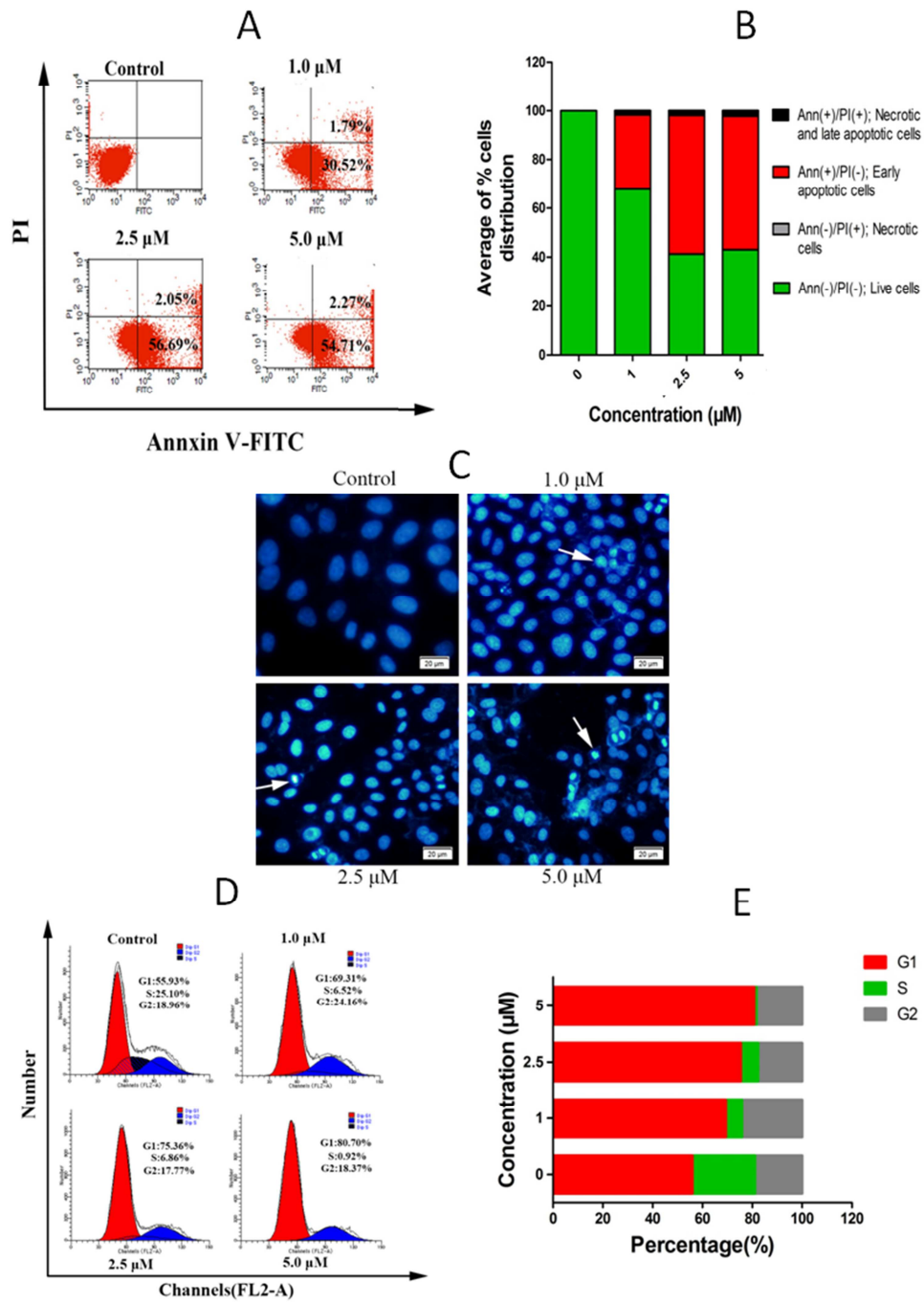


Figure 5

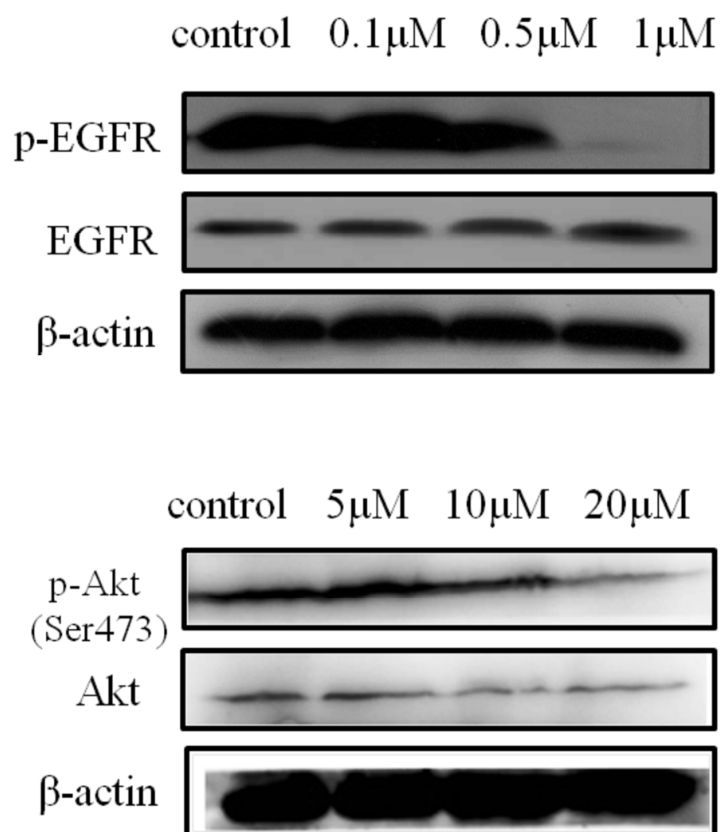
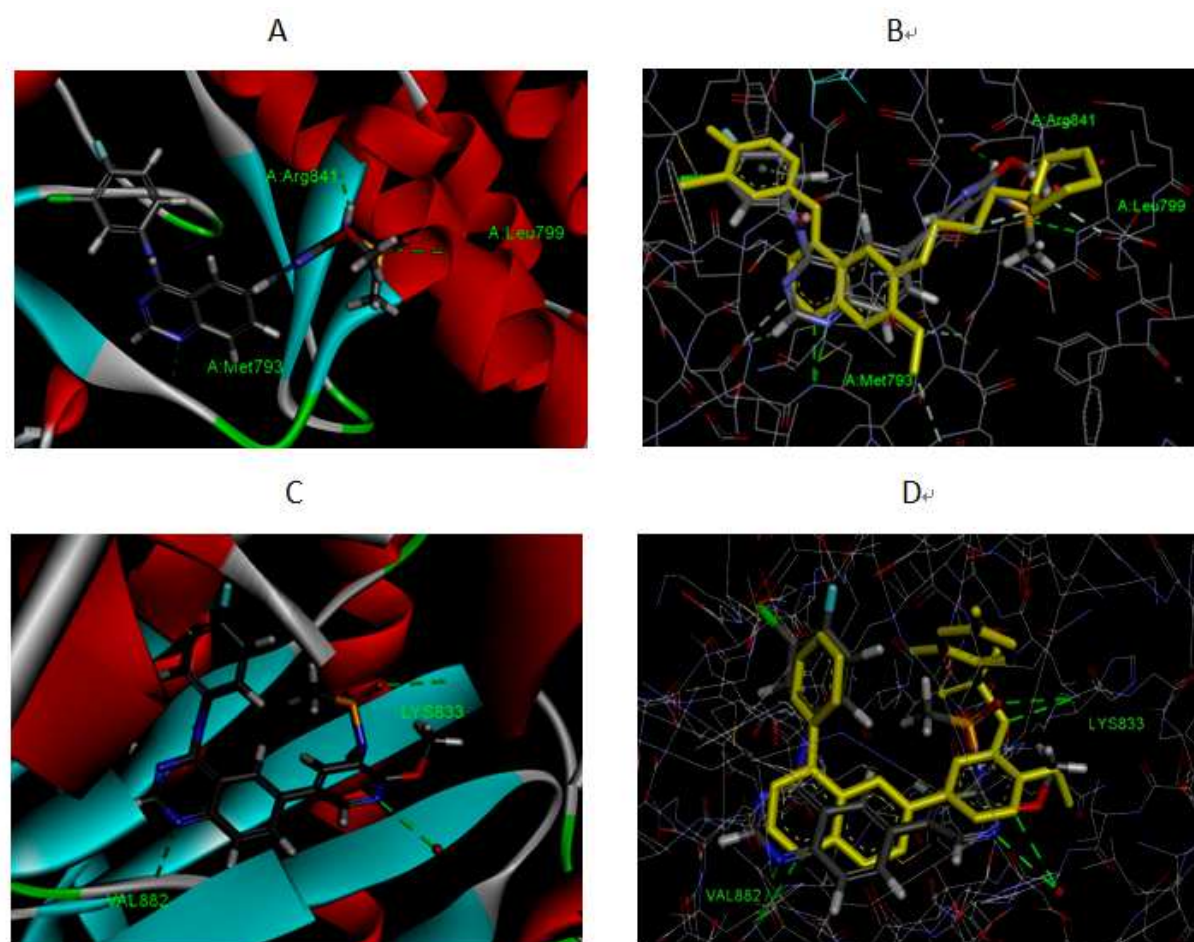
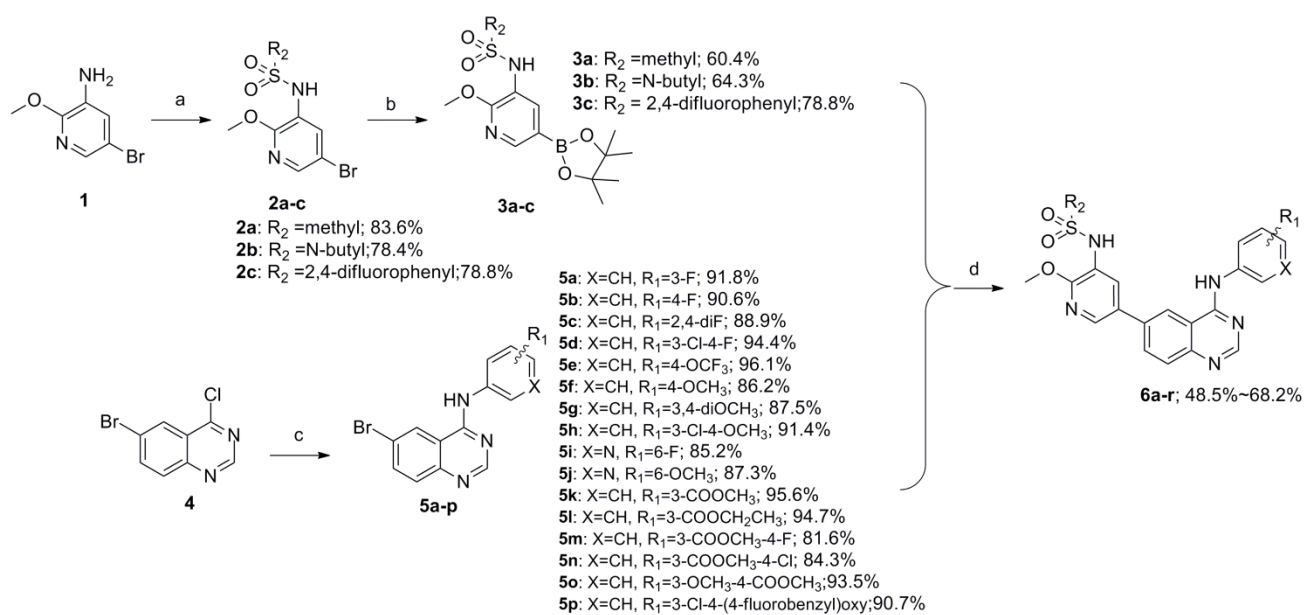


Figure 6



Scheme 1



A series of 4-aminoquinazolines derivatives containing 6-sulfonamide substituted pyridyl group were synthesized.

4-Aminoquinazolines derivatives acted as potent EGFR and PI3K α dual inhibitors.

Compound **6c** and **6i** could be as potential dual inhibitors of EGFR and PI3K α .

Compound **6c** could induce cell cycle arrest in G1 phase and apoptosis in BT549 cells.